

徐璐璐, 柴凤梅, 李强, 等. 东天山沙泉子铁铜矿区火山岩地球化学特征、锆石U-Pb年龄及地质意义[J]. 中国地质, 2014, 41(6): 1771–1790.
Xu Lulu, Chai Fengmei, Li Qiang, et al. Geochemistry and zircon U-Pb age of volcanic rocks from the Shaquanzi Fe-Cu deposit in East Tianshan Mountains and their geological significance[J]. Geology in China, 2014, 41(6): 1771–1790(in Chinese with English abstract).

东天山沙泉子铁铜矿区火山岩地球化学特征、锆石U-Pb年龄及地质意义

徐璐璐¹ 柴凤梅¹ 李 强² 曾 红¹ 耿新霞² 夏 芳¹ 邓 刚³

(1.新疆大学,新疆中亚造山带大陆动力学与成矿预测实验室,新疆 乌鲁木齐 830049;2.中国地质科学院矿产资源研究所国土资源部成矿作用与资源评价重点开放实验室,北京 100037;3.新疆地质矿产局第六地质大队,新疆 哈密 839000)

提要:沙泉子铁铜矿床是东天山地区赋存于火山岩中的矿床之一。矿体产于底坎尔组玄武岩与英安岩接触部位,在闪长玢岩与围岩接触带上也可见不规则铁矿化。对火山岩的形成时代以及构造地质背景的研究是重建成矿过程的关键。LA-ICP-MS 锆石U-Pb定年结果表明,沙泉子铁铜矿区底坎尔组流纹岩和闪长玢岩的 $^{206}\text{Pb}/^{238}\text{U}$ 加权平均年龄分别为 $(321.7\pm1.7)\text{Ma}$ 和 $(322.2\pm1.7)\text{Ma}$,是早石炭世末岩浆活动的产物。元素地球化学和Hf同位素特征表明,底坎尔组火山岩属钙碱性系列,富集轻稀土元素(LREE)和大离子亲石元素(LILE),亏损高场强元素(Nb、Ta、Ti),具有岛弧火山岩地球化学特征。基性岩来源于受俯冲板片流体交代的亏损地幔,中性岩为基性岩分离结晶的产物,流纹岩是新生地壳物质部分熔融形成。综合前人研究成果表明,沙泉子铁铜矿床形成于早石炭世末陆缘弧环境,铁矿化不早于322 Ma。

关 键 词:锆石U-Pb年龄;Hf同位素;流纹岩;沙泉子铁铜矿;东天山

中图分类号:P597;P588.1;P618.31 **文献标志码:**A **文章编号:**1000-3657(2014)06-1771-20

东天山是中亚成矿域的重要组成部分,具有极为复杂的地质演化过程,也是中国最重要的铁矿、有色金属和铜镍矿床成矿带之一^[1-6],因此长期以来一直是国内外地质学家研究的热点地区之一。东天山地区广泛分布着石炭纪火山岩,是重建东天山造山带构造格局的重要研究对象,但是岩石成因及产出的构造环境存有多种争议,如是大规模裂谷事件的产物^[7,8]和洋壳俯冲产生的岩浆弧^[9-11]。近年来,产于火山岩中的铁矿床勘查在新疆北部取得重大进展,并被列为中国富铁矿的重要类型之一(如阿尔泰的大型蒙库铁矿床、西天山的查岗诺尔铁矿、

东天山的雅满苏铁矿等)^[12]。然而该类型矿床的成因和成矿机制等问题长期以来未有定论。东天山地区发育多个产于石炭纪火山岩中的铁矿床(如雅满苏铁矿,沙泉子铁铜矿床、红云滩铁矿床、百灵山铁矿床等),对这些矿床的形成时代、成矿地球动力学背景以及成矿过程等有不同的认识^[13-21]。赋矿火山岩的形成时代、地球化学属性以及形成环境是研究这些问题的关键之一。

沙泉子铁铜矿床是20世纪70年代发现的赋存于石炭纪火山岩中的铁多金属矿床,前人对沙泉子铁铜矿床的地质特征和含矿岩石开展过研究,对矿床形成

收稿日期:2014-10-09;改回日期:2014-10-29

基金项目:国土资源部公益性行业科研专项经费项目(201211073-03)和国家重点基础研究发展计划“973”项目(2012CB416803)联合资助。

作者简介:徐璐璐,女,1989年生,硕士生,矿物学、岩石学、矿床学专业;E-mail:356725316@qq.com。

通讯作者:柴凤梅,女,1971年生,教授,主要从事岩石学、矿床学的教学与研究工作;E-mail:chafengmei@163.com。

时代(126~300 Ma)和成因认识有较大差异^[19~22],如对矿床成因有火山热液^[13]、火山喷发晚期(或喷发期后)与火山侵入岩有关的气液交代-充填^[14]、矿浆喷溢灌入^[15]、接触变质火山沉积^[18]、矽卡岩化^[19]等的不同认识。

鉴于此,本文对东天山沙泉子铁铜矿区底坎尔组火山岩和与成矿有密切关系的闪长玢岩开展年代学及地球化学研究,探讨它们精确的形成时代、形成机制及演化过程,为沙泉子铁铜矿床的形成时代和成因提供重要依据,为区域上石炭纪火山岩研究提供新的年代学和地球化学资料,为该区的古生代构造演化提供新的信息。

1 区域及矿床地质

东天山是天山造山带的东延部分,夹持于哈萨克斯坦—准噶尔板块与塔里木板块之间。近东西向的康古尔断裂、秋明塔格—苦水断裂(雅满苏断裂)和阿奇克库都克—沙泉子断裂(中天山北缘断裂)将东天山觉罗塔格构造带分为4个构造-成矿带,即大南湖头苏泉带、小热泉子—梧桐窝子带、康古尔塔格带和阿齐山—雅满苏带^[3]。其中阿齐山—雅满苏带分布有众多产于石炭纪火山岩中的铁铜多金属矿床(如红云滩铁矿床、百灵山铁矿床、铁岭铁矿床、雅满苏铁铜矿床、沙泉子铁铜矿床和黑峰山铁(铜)矿床等)。带内主要有下石炭统阿奇山组、雅满苏组、底坎尔组(又名沙泉子组)、马头滩组,上石炭统土古土布拉克组、二叠系哈尔加乌组和阿尔巴萨依组以及第四系沉积物^[5]。其中阿奇山组为近火山口相的中性-酸性火山岩组合;雅满苏组以生物灰岩和碎屑岩为主,间夹少量基性-中酸性火山岩组合;底坎尔组以中薄层状灰岩和碎屑岩为主,夹中酸性火山岩组合;马头滩组为中基性为主的火山岩组合;土古土布拉克组为火山岩夹碎屑岩组合^[23]。哈尔加乌组和阿尔巴萨依组为陆相火山岩组合。在带内华力西期和印支期花岗岩广为发育,主要有花岗闪长岩、二长花岗岩、钾长花岗岩以及少量闪长岩和碱性花岗岩等(图1-a)。

沙泉子铁铜矿床位于新疆哈密市南东约180 km处,阿齐山—雅满苏带东段。矿区出露地层为早石炭世末底坎尔组火山-沉积岩和第四系沉积物。根据岩性特征底坎尔组可分为四个岩性段:第一岩

性段为石灰岩和砂岩夹英安岩和砂质凝灰岩组合,英安岩中发育透镜状铁矿体和蚀变带;第二岩性段为英安岩-流纹岩-玄武岩-凝灰岩夹石灰岩和砂岩组合;第三岩性段为基-中-酸性凝灰岩、中酸性火山熔岩夹玄武岩组合,脉岩、断裂较发育;第四岩性段为凝灰岩-玄武岩夹少量流纹岩组合。第二和第三岩性段是主要含矿层位。矿区内褶皱强烈,断裂发育,主构造线呈北东向,控制了地层与岩体的产出。矿区内侵入岩以中性岩为主,仅见少量酸性岩,其中矿区西部和北部出露有规模较大的闪长岩体,中部为出露面积不大的细粒闪长岩和石英闪长岩。脉岩极为发育,多沿断裂构造侵位,其中闪长玢岩脉有早晚两期,其中早期闪长玢岩被晚期闪长岩脉和花岗斑岩脉穿切,晚期闪长玢岩切穿所有地质体。沙泉子铁铜矿区分东、中、西三个矿段,各矿段地质特征相似,属于同一含矿带,仅由于断层或岩体相隔,矿床主要集中在中矿段。矿体产于底坎尔组第二和第三岩性段之间的玄武岩和英安岩接触部位,在闪长玢岩与围岩接触带上也可见不规则铁矿化(图1-b)。矿体总体与地层的产状一致,主要呈层状、似层状及透镜状产出,倾向南,倾角较缓,地表出露为铁矿,未见原生铜矿体,仅见有零星的孔雀石。围岩蚀变不均匀,西矿段和东矿段蚀变弱,中矿段蚀变强烈,尤其在与闪长玢岩脉体接触部位蚀变发育,主要有石榴石化、绿帘石化、绿泥石化、钾长石化、碳酸盐化和硅化,几种蚀变无明显分带现象,但一般靠近矿体者,蚀变较强,由此可见,早期闪长玢岩与铁矿体在空间上关系密切。

2 岩相学特征

本研究在沙泉子铁铜矿区实测了地层剖面(图2),主要为中基-酸性火山岩(熔岩和火山碎屑岩)夹碳酸盐岩组合,出露的火山岩主要有玄武岩、安山岩、流纹岩、英安岩和流纹质凝灰岩。在矿区也发育与铁矿床密切相关的闪长玢岩脉,它们的岩相学特征如下:

流纹岩呈灰红色,致密坚硬,碎块呈尖棱角状。斑状结构,流纹构造,斑晶含量为20%~25%,主要由钠长石和石英组成。其中石英多呈熔粒状,个别为自形粒状,裂纹发育,多具波状和镶嵌状消光;钠长石多呈半自形板状,部分晶体破碎,大小约

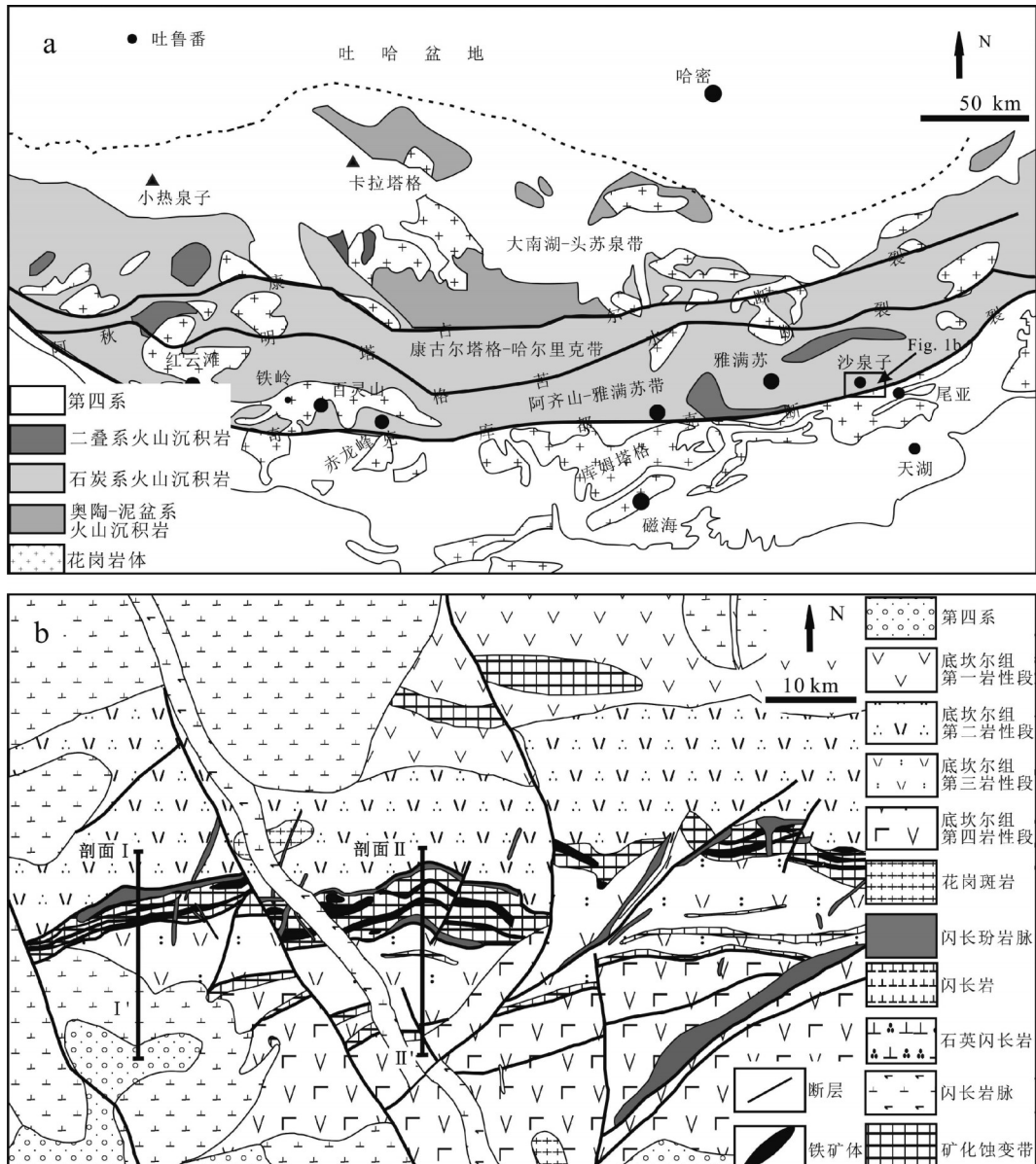


图1 东天山区域地质简图(a)和沙泉子铁铜矿床矿区地质图(b)(a—据文献[3,24]修编,b—据资料①修编)
 Fig.1 Regional geological sketch map of the East Tianshan Mountains (a) and geological sketch map of the Shaquanzi Fe-Cu deposit (b) (a—modified after reference[3,24]; b—after ①)

$20\mu\text{m} \times 30\mu\text{m}$,个别呈长板状晶约 $60\mu\text{m} \times 100\mu\text{m}$,多已高岭土化、绢云母化而表面浑浊。基质为致密的隐晶质,占85%~90%,微晶镶嵌粒状结构,由镶嵌粒状长石、石英、绢云母、绿泥石等组成(图3-a,b)。

玄武岩呈灰绿色,斑状结构,块状构造。斑晶主要有基性斜长石(10%~15%)和辉石(5%~6%)组

成,其中斜长石斑晶呈自形-半自形晶,多已发生钠黝帘石化蚀变而表面浑浊不清;辉石呈自形晶,多发生绿泥石和绿帘石蚀变。基质(约85%)主要为斜长石、辉石微晶和玻璃质组成。副矿物有绢云母、绿泥石、绿帘石和磁铁矿(图3-c)。

英安岩呈灰白色,斑状结构,块状构造。斑晶

①新疆维吾尔自治区第六地质勘查大队.沙泉子铁铜矿床地质调查报告[R],2012.

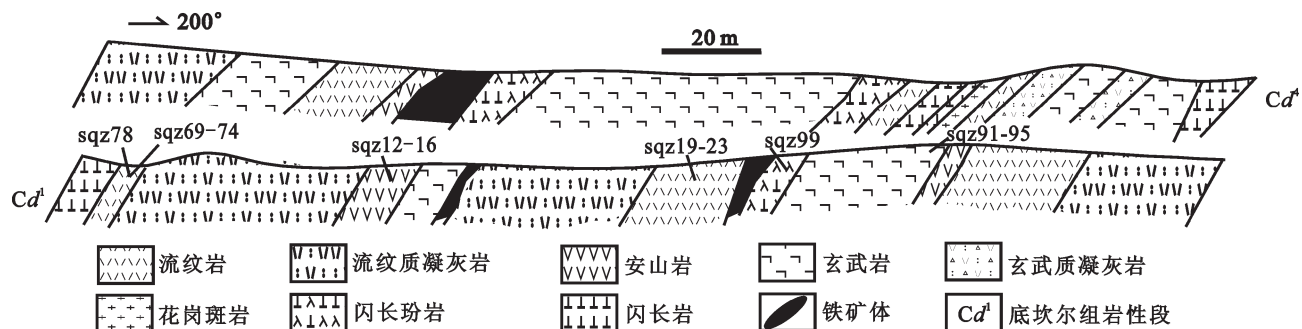


图2 沙泉子铁铜矿区底坎尔组实测剖面及采样位置图

Fig.2 Stratigraphic section of the Dikaner Formation in the Shaquanzi Fe-Cu ore district, showing sampling sites

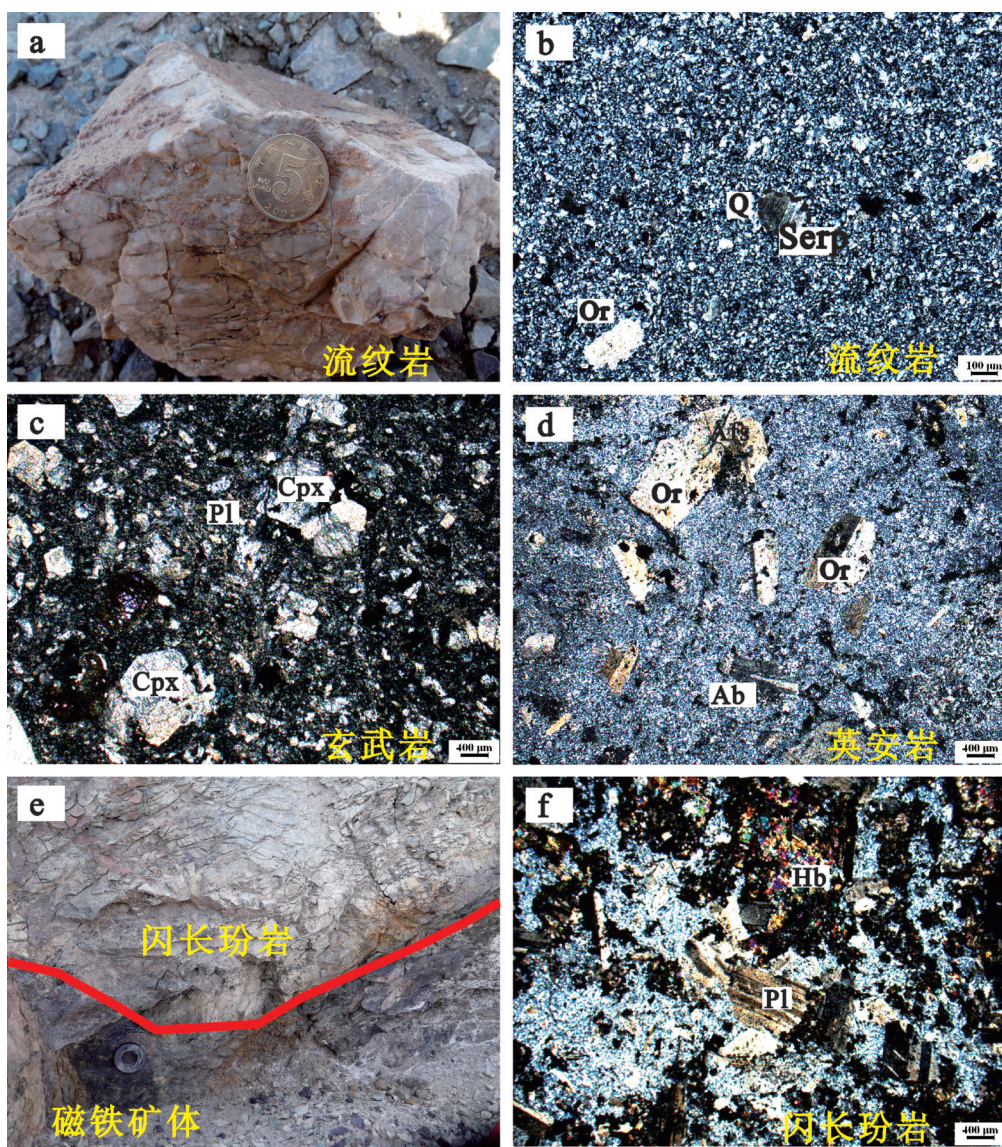


图3 沙泉子铁铜矿区火山岩岩相学特征

Fig.3 Representative photographs of volcanic rocks in the Shaquanzi Fe-Cu ore district, East Tianshan Mountains

约含20%，主要为石英、钾长石和钠长石组成。其中钠长石多呈半自形板状，大小约0.4 mm×0.8 mm，部分晶体破碎；钾长石多呈自形-半自形，个别呈长板状晶约0.8 mm×1 mm，多已高岭土化、绢云母化，表面浑浊(图3-d)。基质为致密的隐晶质，占80%~85%，微晶镶嵌粒状结构，由镶嵌粒状长石、石英、绢云母、绿泥石等组成。

闪长玢岩分布于矿化蚀变带两侧，顺地层产出，受后期热液影响发生蚀变，与磁铁矿直接接触，且接触处见明显的烘烤边。手标本呈浅绿色，斑状结构，块状构造。斑晶主要为斜长石(10%~15%)和普通角闪石(10%)组成，偶见黑云母。其中斜长石自形程度好，聚片双晶发育，表面因蚀变而浑浊不清，角闪石多已蚀变为绿泥石而呈绿色。基质为隐晶质，占80%~85%，主要为斜长石和普通角闪石组成，斜长石自形程度差，大部分角闪石已绿泥石化，少量他形石英充填于其他矿物的间隙内(图3-e,f)。

流纹质凝灰岩呈灰红色，致密坚硬，见暗灰色与肉红色条带相见排列。

3 岩石地球化学特征

本研究采集了沙泉子铁铜矿区底坎尔组6件流纹岩，玄武岩、安山岩和闪长玢岩各5件进行地球化学分析。它们的主量、微量和稀土元素分析在广州澳石分析测试中心测定，结果列于表1。氧化物利用X荧光光谱仪(ME-XRF26)测试，其中 Al_2O_3 、 CaO 、 Fe_2O_3 、 K_2O 、 MgO 、 MnO 、 Na_2O 、 P_2O_5 、 SiO_2 、 TiO_2 采用GB/T14506.28-2010标准； H_2O^+ 按GB/T14506.2-2010标准； CO_2 按GB9835-1988标准； FeO 用滴定法测定，按照GB/T14506.14-2010标准执行； LOI 采用LY/T1253-1999标准。微量元素用四酸消解、质谱/光谱仪综合分析(ME-MS61)，稀土元素采用硼酸锂熔融、等离子质谱法(ME-MS81)测定。

3.1 主量元素

沙泉子铁铜矿区火山岩的 SiO_2 含量介于76.0%~79.6%，45.9%~48.6%和53.4%~54.8%，在火山岩的 SiO_2 - Zr/TiO_2 图上(图4)，位于流纹岩、安山岩和玄武岩区，显示了基性-中性-酸性连续岩石系列。所有火山岩的全碱含量($\text{Na}_2\text{O}+\text{K}_2\text{O}$)较高，介于4.93%~7.09%， K_2O 和 Na_2O 含量变化不大且明显富钠

($\text{Na}_2\text{O}>\text{K}_2\text{O}$)。 TiO_2 含量极低，介于0.17%~1.11%。除2件玄武岩样品的里特曼指数(σ)达4.6和5.1外，大多数样品的里特曼指数小于3.3，表明属钙碱性岩石。流纹岩的铝饱和指数(A/CNK)为0.88~0.92，显示了铝不饱和特征。闪长玢岩与安山岩具有相似的主量元素特征，即具有中等的 SiO_2 (52.0%~59.2%)和 CaO (5.98%~12.55%)含量；高的 MgO (3.16%~4.44%)、 TFeO (4.04%~8.10%)、 Al_2O_3 (16.55%~17.85%)含量；低的 TiO_2 (0.64%~0.84%)和 P_2O_5 (0.08%~0.15%)含量；全碱含量高(4.74%~7.81%)且明显富钠(Na_2O 含量> K_2O 含量)。样品的 Mg^+ 介于0.47~0.69，铝饱和指数(A/CNK)为0.58~1.02，属铝不饱和岩石。基性和中性岩的 SiO_2 与 Na_2O 、 Al_2O_3 、 MgO 、 CaO 和 TFeO 具有良好的负相关性(图略)，表明岩浆可能经历了结晶分异演化作用。

3.2 微量和稀土元素

所有火山岩的稀土元素总量(ΣREE)变化不大，介于 42.85×10^{-6} ~ 84.02×10^{-6} 。在球粒陨石标准化配分模式图上，所有岩石表现为轻稀土轻微富集($(\text{La/Yb})_{\text{N}} = 2.21 \sim 5.16$)的右倾型，流纹岩具有明显的Eu负异常($\delta \text{Eu} = 0.40 \sim 0.46$)，其余样品呈现不明显的Eu异常($\delta \text{Eu} = 0.89 \sim 1.07$) (图5-a)。在原始地幔标准化蛛网图上(图5-b)，所有样品体现了相似的岛弧火山岩的地球化学特征，即亏损高场强元素(Nb、Ta、Ti)，不同程度地富集大离子亲石元素(K、Th和Rb)。所有的流纹岩样品具有明显的Sr负异常，说明岩浆发生了斜长石的分离结晶作用或者部分熔融过程中有斜长石的残留。

闪长玢岩的稀土元素总量(ΣREE)变化于 65.38×10^{-6} ~ 161.45×10^{-6} ，球粒陨石标准化稀土元素配分图上呈现轻稀土富集($(\text{La/Yb})_{\text{N}} = 2.9 \sim 15.6$)的右倾型，并具有轻微的Eu正异常($\delta \text{Eu} = 1.02 \sim 1.27$) (图5-a)。所有样品在原始地幔标准化蛛网图上(图5-b)呈现一致的曲线分布形式，与矿区的中性和基性火山岩具有相似特征，即亏损高场强元素(Nb、Ta、Ti)，不同程度地富集大离子亲石元素(K、Th和Rb)的岛弧火山岩特征。

4 LA-ICP-MS锆石U-Pb定年

本研究对沙泉子铁铜矿区底坎尔组流纹岩(sqz78)和矿区闪长玢岩(sqz99)进行了年龄测定，

表1 沙泉子铁铜矿区火山岩和闪长玢岩的主量(%)和微量(10^{-6})元素组成Table 1 Major (%) and trace (10^{-6}) element data of the volcanic rocks and diorite–porphyrite in the Shaquanzi Fe–Cu ore district, East Tianshan Mountains

样品原号	sqz69	sqz70	sqz71	sqz72	sqz73	sqz74	sqz19	sqz20	sqz21	sqz22	sqz23
岩石类型	流纹岩						闪长玢岩				
SiO ₂	76.00	79.60	78.40	79.20	78.60	77.70	55.40	54.00	58.50	59.20	52.00
TiO ₂	0.35	0.28	0.28	0.17	0.19	0.26	0.71	0.72	0.84	0.71	0.64
Al ₂ O ₃	12.30	10.90	11.45	11.05	11.70	11.80	17.55	17.40	17.85	16.55	17.40
Fe ₂ O ₃	0.73	0.69	0.67	0.50	0.49	0.54	4.85	4.21	3.10	3.85	6.72
FeO	0.66	0.58	0.48	0.41	0.72	0.59	1.97	1.56	1.25	2.12	2.05
MnO	0.02	0.01	0.02	0.01	0.01	0.01	0.15	0.15	0.12	0.11	0.19
MgO	0.25	0.18	0.22	0.19	0.15	0.18	3.81	3.53	3.16	4.44	3.73
CaO	1.38	1.16	1.24	1.08	0.94	1.12	7.90	9.62	5.98	6.02	12.55
Na ₂ O	7.02	6.19	6.53	6.37	6.74	6.78	6.11	5.82	7.36	6.73	4.36
K ₂ O	0.07	0.06	0.06	0.06	0.06	0.06	0.54	0.62	0.45	0.69	0.38
P ₂ O ₅	0.12	0.08	0.08	0.05	0.06	0.09	0.10	0.08	0.15	0.12	0.11
LOI	1.07	0.94	1.09	0.84	0.66	0.87	2.94	3.38	2.05	1.20	2.06
Total	99.31	100.09	100.04	99.52	99.60	99.41	100.06	99.53	99.56	99.62	100.14
A/NK	1.06	1.07	1.07	1.05	1.06	1.06	1.66	1.71	1.43	1.41	2.31
A/CNK	0.88	0.89	0.88	0.89	0.92	0.90	0.71	0.63	0.77	0.73	0.58
Sc	3.50	2.60	3.30	2.40	2.60	3.10	26.80	30.10	25.40	27.90	27.80
V	18.00	13.00	14.00	9.00	8.00	13.00	194.00	195.00	147.00	162.00	236.00
Cr	20.00	20.00	20.00	30.00	30.00	30.00	50.00	60.00	30.00	60.00	60.00
Co	1.30	0.80	0.90	0.60	0.60	0.70	7.00	5.40	4.30	5.00	4.90
Ni	2.30	1.80	1.40	1.00	0.80	1.00	7.30	5.50	5.40	8.70	6.70
Cu	7.80	5.90	7.40	5.50	4.10	5.40	78.00	4.10	<0.2	0.70	1.00
Zn	11.00	7.00	10.00	10.00	8.00	7.00	66.00	66.00	59.00	61.00	51.00
Ga	10.10	8.74	9.44	8.89	8.76	9.64	15.85	17.25	12.50	14.55	25.00
Rb	0.80	0.50	0.30	0.20	0.20	0.20	5.80	6.90	5.70	8.10	7.60
Sr	33.20	28.90	25.50	28.70	26.20	48.30	464.00	437.00	294.00	312.00	570.00
Y	18.10	17.20	17.40	14.00	14.80	15.50	20.80	26.00	24.50	18.90	15.90
Zr	137.00	159.00	180.00	136.00	142.00	157.00	37.00	58.00	69.00	78.00	35.00
Nb	4.90	5.20	5.60	4.30	4.50	5.50	1.70	1.60	2.30	2.40	1.00
Mo	1.31	1.83	1.37	1.15	1.15	1.73	0.64	0.65	0.56	0.68	0.86
Ba	19.30	13.10	11.30	10.40	11.40	11.50	185.50	191.00	131.00	225.00	91.30
Hf	2.60	3.30	3.70	3.10	3.30	3.50	0.90	0.90	1.60	1.80	0.90
Ta	0.20	0.30	0.30	0.20	0.20	0.20	0.20	0.20	0.20	0.20	0.10
Pb	2.00	1.30	1.40	0.50	0.60	2.20	23.40	26.60	9.70	10.40	17.40
Th	6.20	8.10	9.80	6.70	7.90	8.20	0.70	0.80	1.80	2.40	1.50
U	1.90	2.00	2.20	1.60	1.70	2.10	2.40	2.30	2.00	2.90	3.20
La	11.80	9.90	15.90	6.10	5.70	8.00	11.90	14.20	12.70	8.10	32.90
Ce	28.40	24.30	34.40	16.90	15.90	20.10	26.00	31.00	27.60	22.10	68.10
Pr	3.82	3.20	4.00	2.14	2.04	2.84	3.46	4.02	3.60	3.22	8.16
Nd	15.30	12.70	15.40	8.70	8.40	11.30	15.10	16.90	16.00	14.40	32.80
Sm	3.46	2.81	3.00	1.93	1.92	2.46	3.52	3.65	4.25	3.55	5.63
Eu	0.43	0.34	0.40	0.26	0.26	0.29	1.51	1.45	1.46	1.27	1.89
Gd	2.78	2.26	2.34	1.85	1.68	2.03	3.74	4.55	4.40	3.68	4.16
Tb	0.44	0.38	0.38	0.29	0.27	0.34	0.59	0.72	0.68	0.53	0.51
Dy	3.08	2.57	2.74	2.08	2.16	2.52	3.81	4.41	4.41	3.15	3.01
Ho	0.64	0.59	0.60	0.46	0.50	0.55	0.77	0.92	0.93	0.67	0.58
Er	1.97	1.85	1.96	1.48	1.59	1.81	2.28	2.80	2.75	2.13	1.72
Tm	0.33	0.33	0.34	0.27	0.29	0.32	0.31	0.36	0.40	0.28	0.25
Yb	2.04	2.07	2.21	1.67	1.85	2.01	1.92	2.25	2.52	2.00	1.51
Lu	0.29	0.33	0.35	0.26	0.29	0.32	0.28	0.34	0.34	0.30	0.23
Σ REE	74.78	63.63	84.02	44.39	42.85	54.89	75.19	87.57	82.04	65.38	161.45
LREE/HREE	5.46	5.13	6.69	4.31	3.97	4.54	4.49	4.36	3.99	4.13	12.49
(La/Yb)n	4.15	3.43	5.16	2.62	2.21	2.85	4.45	4.53	3.61	2.91	15.63
δ Eu	0.42	0.41	0.46	0.42	0.44	0.40	1.27	1.09	1.03	1.07	1.19

续表1

样品原号	sqz12	sqz13	sqz14	sqz15	sqz16	sqz91	sqz92	sqz93	sqz94	sqz95
岩石类型	安山岩					玄武岩				
SiO ₂	54.80	53.40	53.60	53.90	54.10	48.60	48.10	47.90	45.90	46.00
TiO ₂	0.62	0.62	0.61	0.62	0.63	0.93	0.94	0.89	1.12	1.11
Al ₂ O ₃	18.65	18.20	18.25	18.40	18.50	14.20	14.30	13.30	14.90	14.90
Fe ₂ O ₃	8.06	7.97	7.91	8.04	8.07	10.17	10.26	10.26	10.16	9.95
FeO	3.55	3.65	3.51	3.86	3.54	5.84	6.00	5.24	5.26	4.95
MnO	0.17	0.17	0.17	0.17	0.15	0.39	0.40	0.35	0.39	0.38
MgO	3.59	3.53	3.44	3.51	3.54	9.60	9.50	10.50	7.47	7.08
CaO	5.31	5.72	5.39	5.43	4.90	7.62	7.65	8.81	8.37	9.17
Na ₂ O	3.83	2.95	3.89	3.86	2.92	2.07	2.04	1.90	2.34	2.38
K ₂ O	2.17	2.59	2.20	2.18	2.74	2.42	2.43	1.70	2.81	2.55
P ₂ O ₅	0.17	0.16	0.16	0.16	0.16	0.28	0.29	0.26	0.27	0.27
LOI	2.98	3.72	3.66	3.31	3.89	3.53	3.64	3.65	6.03	5.88
Total	100.92	98.96	99.13	100.13	99.25	102.12	101.91	101.11	98.99	98.74
A/NK	2.17	2.39	2.09	2.13	2.40	2.37	2.40	2.70	2.18	2.25
A/CNK	1.03	1.01	0.99	1.00	1.12	0.72	0.72	0.64	0.68	0.64
Sc	17.40	18.10	18.80	18.00	15.70	37.50	38.60	34.60	35.80	35.60
V	222.00	220.00	211.00	216.00	216.00	296.00	303.00	295.00	319.00	318.00
Cr	10.00	10.00	10.00	10.00	10.00	650.00	650.00	810.00	270.00	260.00
Co	20.90	20.80	20.10	21.60	20.80	41.50	43.70	45.60	36.10	35.10
Ni	8.40	8.20	7.50	8.40	8.00	100.50	104.50	136.00	75.10	73.20
Cu	71.10	68.40	67.20	75.80	67.90	92.00	102.00	93.10	34.00	53.50
Zn	97.00	100.00	98.00	100.00	104.00	362.00	379.00	257.00	299.00	282.00
Ga	18.70	18.60	17.90	19.45	18.25	14.40	15.35	14.50	17.00	17.80
Rb	25.60	34.00	37.30	26.10	27.70	54.80	52.90	32.10	57.40	52.20
Sr	527.00	409.00	447.00	504.00	413.00	299.00	309.00	304.00	342.00	390.00
Y	17.20	15.70	15.40	14.80	14.60	23.60	24.50	23.40	25.10	25.80
Zr	65.00	57.00	57.00	56.00	55.00	92.00	96.00	89.00	99.00	102.00
Nb	2.60	2.30	2.20	2.20	2.20	2.20	2.00	1.90	2.30	2.40
Mo	0.48	0.57	0.63	0.47	0.47	0.36	0.31	0.28	0.42	0.61
Ba	371.00	387.00	322.00	349.00	391.00	558.00	554.00	335.00	882.00	809.00
Hf	1.80	1.60	1.70	1.70	1.70	2.70	2.80	2.60	2.60	2.70
Ta	0.40	0.30	0.20	0.20	0.20	0.12	0.12	0.11	0.15	0.16
Pb	9.70	8.50	7.60	8.50	8.90	13.00	13.30	15.80	34.00	43.30
Th	1.50	1.19	1.22	1.14	1.18	1.66	1.74	1.57	1.21	1.20
U	0.97	0.47	0.50	0.42	0.44	1.57	1.44	1.59	0.74	0.79
La	9.70	7.60	7.70	7.20	7.30	8.60	9.00	7.90	9.20	9.50
Ce	20.30	16.60	17.00	15.60	15.90	25.40	26.10	24.00	26.10	27.20
Pr	2.61	2.29	2.25	2.16	2.16	3.56	3.76	3.37	3.66	3.74
Nd	11.40	10.20	10.10	10.00	9.70	17.20	17.90	16.30	17.10	17.30
Sm	2.73	2.74	2.55	2.40	2.60	4.76	4.81	4.58	4.63	4.87
Eu	0.94	0.92	0.89	0.90	0.92	1.45	1.43	1.39	1.44	1.55
Gd	3.04	2.67	2.80	2.76	2.65	4.80	5.04	4.72	4.74	4.73
Tb	0.46	0.41	0.44	0.40	0.40	0.72	0.74	0.66	0.72	0.72
Dy	2.95	2.73	2.64	2.62	2.55	4.31	4.40	4.16	4.44	4.54
Ho	0.61	0.56	0.55	0.54	0.53	0.82	0.87	0.81	0.88	0.92
Er	1.92	1.71	1.63	1.67	1.65	2.38	2.46	2.29	2.57	2.59
Tm	0.27	0.30	0.27	0.25	0.26	0.35	0.38	0.36	0.40	0.40
Yb	1.65	1.65	1.67	1.62	1.71	2.12	2.22	2.16	2.31	2.31
Lu	0.28	0.25	0.25	0.24	0.25	0.33	0.35	0.31	0.35	0.35
ΣREE	58.86	50.63	50.74	48.36	48.58	76.80	79.46	73.01	78.54	80.72
LREE/HREE	4.26	3.93	3.95	3.79	3.86	3.85	3.83	3.72	3.79	3.87
(La/Yb)n	4.22	3.30	3.31	3.19	3.06	2.91	2.91	2.62	2.86	2.95
δ Eu	1.00	1.04	1.02	1.07	1.07	0.93	0.89	0.91	0.94	0.99

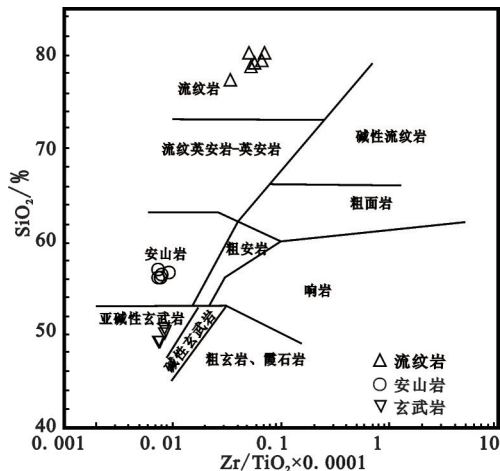


图4 沙泉子铁铜矿区火山岩的SiO₂-Zr/TiO₂图
(据文献[25])

Fig.4 Whole-rock SiO₂ versus Zr/TiO₂ diagram of the volcanic rocks in the Shaquanzi Fe-Cu ore district, East Tianshan Mountains (after reference [25])

采样位置见图2。野外观察表明，闪长玢岩侵入流纹岩地层中。用于测年样品的破碎和锆石的挑选工作由廊坊市科大技术服务公司实验室完成，样品(约30 g)经过严格的粉碎、重液分离和磁选，再在双目镜下挑选出晶形好、无裂缝、干净透明的锆石晶体。锆石样品靶的制作和锆石阴极发光照相在北京锆年领航科技有限公司中心完成。锆石U-Pb定年测试分析在中国地质科学院矿产资源研究所MC

-ICP-MS实验室完成。所用仪器为Finnigan Neptune型MC-ICP-MS及与之配套的Newwave UP 213激光剥蚀系统。激光剥蚀所用束斑直径为25 μm，频率为10 Hz，能量密度约为2.5 J/cm²，以He为载气。详细分析原理和流程可参考文献[27]。每5~7个样品点测定一次标准锆石(GJ-1和Plesovice)，用于观察仪器的状态以保证测试的精确度。样品的同位素比值和元素含量计算采用ICP-MS-DataCal 4.3程序处理^[28]，年龄计算及谐和图的绘制采用Isoplot 3.0^[29]软件处理。单次测量数据点的误差为1σ。普通铅根据实测²⁰⁴Pb校正，年龄值选用²⁰⁶Pb/²³⁸U年龄，其加权平均值具有95%的置信度。

底坎尔组流纹岩样品和闪长玢岩样品的锆石多呈无-浅褐黄色，半自形-自形的长柱状及双锥状晶体，晶棱及晶面清楚。流纹岩中锆石颗粒相对较大，长轴多变化于140~180 μm，长短轴比一般为1:1~2:1。闪长玢岩中锆石长轴多变化于50~120 μm，长短轴比介于1:1~1.5:1。大部分锆石具有岩浆锆石的生长环带，个别锆石含有不透明的包裹体，也有个别锆石颗粒见有核边结构，核部呈浑圆状(sqz78中点6.1, 14.1, 20.1和sqz99中点2.1)，可能为喷发过程中捕获的或者继承的残留锆石，边部颜色均匀，震荡环带发育，且核部与边部接触界线规则(图6)。样品的LA-ICP-MS锆石U-Pb年龄分析结果列于表1。

流纹岩中锆石的U含量分布在15.8×10⁻⁶~216×

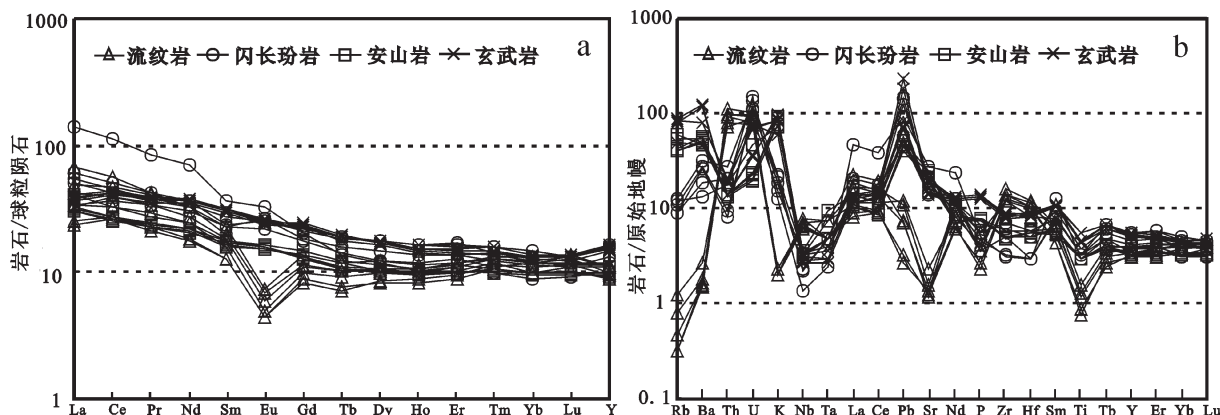


图5 沙泉子铁铜矿区火山岩和闪长玢岩的稀土元素球粒陨石标准化配分模式图(a)和微量元素原始地幔配分模式图(b)(原始地幔值和球粒陨石值据资料[26])

Fig.5 Chondrite-normalized REE patterns (a) and primitive mantle-normalized trace elements patterns (b) for the volcanic rocks and diorite-porphyrite in the Shaquanzi Fe-Cu ore district, East Tianshan Mountains (normalized values after reference [26])

表2 沙泉子铁铜矿区流纹岩和闪长玢岩 LA-ICP-MS 锆石 U-Pb 年龄测定结果
Table 2 LA-ICP-MS zircon dating results of the rhyolite and diorite-porphyry in the Shaqueanzi Fe-Cu ore district, East Tianshan Mountains

测点	元素含量及比值	同位素比值						样品编号: sqz78	年龄/Ma							
		Pb/10 ⁻⁶	²³⁸ U/10 ⁻⁶	²³² Tb/10 ⁻⁶	²³² Rh/ ²³⁸ U	²⁰⁷ Pb/ ²⁰⁶ Pb	²⁰⁷ Pb/ ²³⁵ U	²⁰⁶ Pb/ ²³⁸ U	²⁰⁷ Pb/ ²⁰⁶ Pb	²⁰⁷ Pb/ ²³⁵ U	²⁰⁶ Pb/ ²³⁸ U	²⁰⁶ Pb/ ²³⁵ U	²⁰⁶ Pb/ ²³⁸ U	1 σ 测值	1 σ 测值	1 σ 测值
1.1	967.71	175.09	359.93	2.06	0.05433	0.00052	0.38035	0.00458	0.05082	0.00041	383.4	20.4	327.3	3.4	319.5	2.5
2.1	206.04	75.85	77.46	1.02	0.05439	0.00103	0.38191	0.00792	0.05103	0.00052	387.1	42.6	328.4	5.8	320.8	3.2
3.1	453.75	87.40	167.35	1.91	0.05209	0.00155	0.36828	0.01089	0.05132	0.00065	300.1	73.1	318.4	8.1	322.6	4.0
4.1	2129.75	216.06	698.52	3.23	0.05481	0.00050	0.38147	0.00369	0.05056	0.00031	405.6	25.0	328.1	2.7	317.9	1.9
5.1	331.80	86.89	95.48	1.10	0.05400	0.00111	0.37980	0.00775	0.05116	0.00064	372.3	46.3	326.9	5.7	321.7	3.9
6.1	222.51	98.65	73.02	0.74	0.05532	0.00070	0.38821	0.00562	0.05097	0.00042	433.4	27.8	333.1	4.1	320.5	2.6
7.1	400.85	23.14	32.03	1.38	0.06727	0.00292	0.47331	0.0214	0.05173	0.00133	855.6	123.1	393.5	15.3	325.1	8.1
8.1	122.03	29.12	29.88	1.03	0.05476	0.00253	0.39152	0.02306	0.05159	0.00196	466.7	103.7	335.5	16.8	324.3	12.0
9.1	264.92	35.33	33.02	0.93	0.06455	0.00238	0.45748	0.02299	0.05128	0.00154	761.1	77.8	382.5	16.0	322.4	9.4
10.1	333.60	25.94	22.39	0.86	0.07551	0.00104	1.71196	0.04441	0.16514	0.00419	1083.3	27.8	1013.0	16.6	985.3	23.2
11.1	187.40	15.18	23.42	1.54	0.05277	0.00547	0.36896	0.03768	0.05095	0.00214	320.4	237.0	318.9	28.0	320.4	13.1
12.1	389.67	55.80	62.10	1.11	0.06815	0.00111	0.51266	0.01145	0.05454	0.00079	872.2	33.3	420.2	7.7	342.3	4.8
13.1	0.56	25.01	21.06	0.84	0.05599	0.00331	0.38981	0.03123	0.05131	0.00423	453.8	133.3	334.2	22.8	322.6	26.0
14.1	447.87	65.11	80.61	1.24	0.05684	0.00088	0.49121	0.00842	0.06290	0.00074	487.1	35.2	405.7	5.7	393.2	4.5
15.1	335.80	59.01	99.62	1.69	0.05549	0.00119	0.38809	0.00826	0.05097	0.00060	431.5	48.1	335.0	6.0	320.5	3.7
16.1	138.82	30.08	25.26	0.84	0.05391	0.00143	0.38048	0.01122	0.05135	0.00079	368.6	63.9	327.4	8.3	322.8	4.8
17.1	129.43	54.47	42.75	0.78	0.05605	0.00142	0.40654	0.01064	0.05276	0.00059	453.8	55.6	346.4	7.7	331.4	3.6
18.1	93.31	41.52	40.99	0.99	0.05599	0.00176	0.39638	0.01299	0.05160	0.00086	453.8	65.7	339.0	9.4	324.3	5.3
19.1	400.56	31.36	34.44	1.10	0.05382	0.00209	0.37809	0.01540	0.05120	0.00118	364.9	88.9	325.6	11.3	321.9	7.2
20.1	1152.46	115.23	225.73	1.96	0.05583	0.00120	0.39297	0.00992	0.05109	0.00074	455.6	50.9	336.5	7.2	321.2	4.5
21.1	1235.88	36.00	35.78	0.99	0.16325	0.00067	10.2642	0.12560	0.45601	0.00516	2500.0	7.9	2458.9	11.3	2421.9	22.8
22.1	128.13	26.30	36.39	1.38	0.05465	0.00142	0.38130	0.01118	0.05083	0.00092	398.2	57.4	328.0	8.2	319.6	5.7
23.1	119.41	25.74	25.18	0.98	0.05608	0.00131	0.38984	0.00948	0.05075	0.00062	457.5	19.4	334.3	6.9	319.1	3.8
24.1	78.13	29.07	18.27	0.63	0.05317	0.00155	0.34383	0.01164	0.04711	0.00089	344.5	66.7	300.1	8.8	296.7	5.5
25.1	0.41	18.41	7.52	0.41	0.05369	0.00457	0.37884	0.03259	0.05141	0.00197	366.7	192.6	326.2	24.0	323.2	12.1
26.1	84.29	34.94	33.38	0.96	0.05427	0.00261	0.37815	0.01632	0.05116	0.00097	383.4	76.8	325.7	12.0	321.6	5.9
27.1	121.63	45.44	36.91	0.81	0.05596	0.00130	0.39097	0.01008	0.05070	0.00062	450.0	51.8	335.1	7.4	318.8	3.8
28.1	207.22	50.66	60.34	1.19	0.05445	0.00351	0.38173	0.02378	0.05109	0.00179	390.8	144.4	328.3	17.5	321.2	11.0
29.1	57.50	24.38	18.71	0.77	0.05314	0.00217	0.34985	0.01533	0.04791	0.00097	344.5	97.2	304.6	11.5	301.7	6.0
30.1	6.26	17.75	15.15	0.85	0.05708	0.00570	0.39777	0.04774	0.05163	0.00428	494.5	222.2	340.0	34.7	324.5	26.2

续表2

测点 ⁵	元素含量及比值			同位素比值			年龄/Ma				
	Pb/10 ⁻⁶	²³⁸ U/10 ⁻⁶	²³² Th/10 ⁻⁶	²³² Th/ ²³⁸ U	²⁰⁷ Pb/ ²⁰⁶ Pb	²⁰⁷ Pb/ ²³⁵ U	²⁰⁷ Pb/ ²³⁸ U	²⁰⁶ Pb/ ²³⁸ U	²⁰⁷ Pb/ ²⁰⁶ Pb	²⁰⁷ Pb/ ²³⁵ U	²⁰⁶ Pb/ ²³⁸ U
	测值	1 σ	测值	1 σ	测值	1 σ	测值	1 σ	测值	1 σ	测值
1.1	471.51	69.73	170.68	2.45	0.06678	0.00062	1.17144	0.01726	0.12728	0.00152	831.5
2.1	167.44	89.34	140.55	1.57	0.05510	0.00076	0.38910	0.00661	0.05125	0.00057	416.7
3.1	105.59	35.63	43.77	1.23	0.05445	0.00256	0.39117	0.02647	0.05202	0.00237	390.8
4.1	155.72	115.41	133.14	1.15	0.05443	0.00073	0.38183	0.00629	0.05095	0.00055	390.8
5.1	17.25	39.00	34.71	0.89	0.05465	0.00195	0.33237	0.01417	0.04043	0.00096	398.2
6.1	80.31	101.50	88.82	0.88	0.05317	0.00108	0.37208	0.00796	0.05105	0.00076	344.5
7.1	7.29	22.92	20.98	0.92	0.05598	0.00481	0.39055	0.03931	0.05115	0.00283	450.0
8.1	57.48	35.33	46.21	1.31	0.05843	0.00283	0.42365	0.03624	0.05225	0.00268	546.3
9.1	20.99	19.92	37.49	1.88	0.06986	0.00261	0.94046	0.04196	0.09834	0.00320	924.1
10.1	250.65	116.15	374.42	3.22	0.05577	0.00070	0.39271	0.00560	0.05122	0.00047	442.6
11.1	15.97	36.14	34.29	0.95	0.05579	0.00230	0.39522	0.01865	0.05148	0.00126	442.6
12.1	0.98	42.34	62.57	1.48	0.05426	0.00194	0.38380	0.01389	0.05183	0.00094	388.9
13.1	94.81	40.12	41.36	1.03	0.09961	0.00075	3.52943	0.05363	0.25742	0.00367	1617.0
14.1	76.12	152.94	171.09	1.12	0.05465	0.00073	0.38954	0.05953	0.05172	0.00042	398.2
15.1	45.89	90.17	94.21	1.04	0.05598	0.00075	0.39941	0.06617	0.05180	0.00041	450.0
16.1	66.51	135.87	89.58	0.66	0.05535	0.00070	0.39035	0.05657	0.05121	0.00042	427.8
17.1	87.18	95.82	134.16	1.40	0.05588	0.00184	0.39551	0.05142	0.05136	0.00085	455.6
18.1	126.10	127.55	186.84	1.46	0.05604	0.00061	0.59916	0.06691	0.06593	0.00061	453.8
19.1	172.35	115.36	306.77	2.66	0.05532	0.00109	0.39398	0.09973	0.05166	0.00081	433.4
20.1	74.56	29.50	35.82	1.21	0.05584	0.00434	0.39577	0.05258	0.05133	0.00142	455.6
21.1	210.14	235.82	129.72	0.55	0.05562	0.00060	0.39498	0.05158	0.05158	0.00050	438.9
22.1	294.08	233.26	333.99	1.43	0.05727	0.00049	0.59401	0.05756	0.07543	0.00060	501.9
23.1	93.74	126.47	195.28	1.54	0.05554	0.00142	0.39076	0.01050	0.05114	0.00085	435.2
24.1	59.77	91.46	124.57	1.36	0.05637	0.00196	0.39703	0.01390	0.05127	0.00098	477.8
25.1	212.24	72.99	87.81	1.20	0.08687	0.00055	2.62822	0.02697	0.21988	0.00213	1366.7
26.1	38.09	65.11	76.87	1.18	0.08829	0.00188	0.63936	0.01505	0.05269	0.00074	1388.6
27.1	108.23	176.54	147.17	0.83	0.05633	0.00082	0.45862	0.00725	0.05936	0.00062	464.9
28.1	76.57	125.09	105.59	0.84	0.05442	0.00070	0.38571	0.05587	0.05121	0.00045	387.1
29.1	347.83	334.47	439.24	1.31	0.05983	0.00041	0.64397	0.06651	0.07820	0.00067	598.2
30.1	125.54	204.64	230.33	1.13	0.05326	0.00051	0.38169	0.0452	0.05208	0.00045	338.9

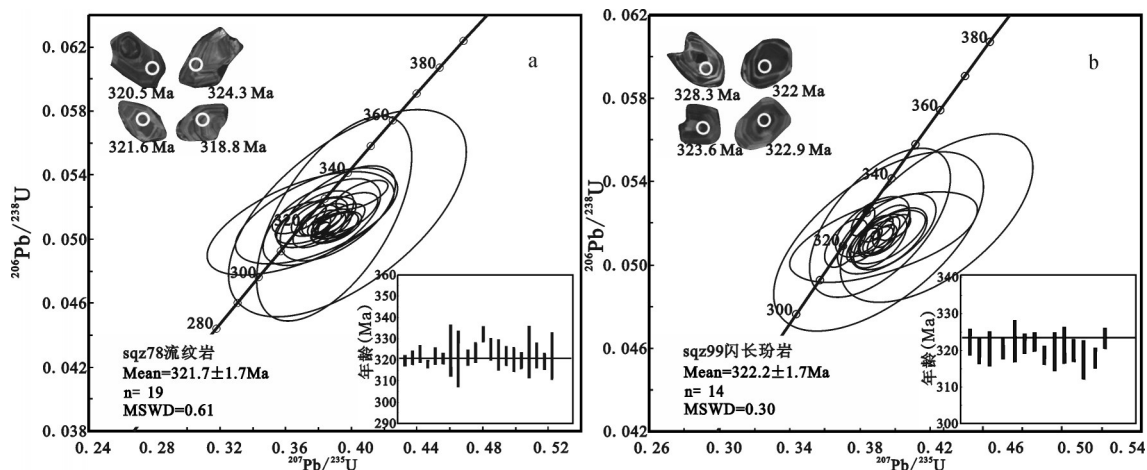


图6 沙泉子铁铜矿区流纹岩和闪长玢岩LA-ICP-MS锆石U-Pb年龄协和图

Fig. 6 LA-ICP-MS zircon U-Pb concordia diagrams of the rhyolite and diorite-porphyrite in the Shaquanzi Fe-Cu ore district, East Tianshan Mountains

10^{-6} , Th含量变化于 $7.52 \times 10^{-6} \sim 359.93 \times 10^{-6}$, Th/U比值介于0.41~3.23,显示了岩浆锆石的Th/U比值典型特征^[30]。除3个样品点(10.1, 14.1, 21.1)年龄结果偏大(985.3 Ma, 393.2 Ma, 2500 Ma),1个样品点年龄结果偏小(296.7 Ma)外,其余19个锆石 $^{206}\text{Pb}/^{238}\text{U}$ 表面年龄数据比较集中,介于317.9~331.4 Ma,在年龄谐和图上聚集在一致线上及其附近一个较小的范围内,表明这些锆石形成后U-Pb体系保持封闭,没有明显的U或Pb同位素的丢失和加入,其加权平均值为(321.7 ± 1.7) Ma(MSWD=0.61)(图6-a),代表了该流纹岩的形成年龄。

闪长玢岩中锆石的U含量介于 $22.9 \times 10^{-6} \sim 235.8 \times 10^{-6}$, Th含量变化于 $20.9 \times 10^{-6} \sim 374.4 \times 10^{-6}$, Th/U比值为0.55~3.22,显示了岩浆锆石的Th/U比值特征^[30]。14个有效分析点的 $^{206}\text{Pb}/^{238}\text{U}$ 表面年龄数据比较集中,介于320.3~328.3 Ma,其加权平均值为(322.2 ± 1.7) Ma(MSWD=0.30)(图6-b),代表了闪长玢岩的结晶年龄。

5 锆石Hf同位素组成

锆石原位Lu-Hf同位素分析在天津地质矿产研究所进行,所用仪器为Finnigan Neptune多接收电感耦合等离子体质谱仪(LA-MC-ICP-MS)及与之配套的Newwave UP 213激光剥蚀系统。激光束斑

直径为 $25 \mu\text{m}$,所用的激光脉冲频率为10 Hz,能量密度约为 2.5 J/cm^2 ,以He为剥蚀物质载气。测定时用锆石国际标样91500作外标。原位Hf同位素比值测定在原U-Pb年龄分析位置或附近进行。相关仪器运行条件及详细分析流程见李怀坤等^[31]。

表3为流纹岩及闪长玢岩中锆石Hf同位素组成。所有测试锆石的 $^{176}\text{Hf}/^{177}\text{Hf}$ 误差值在0.00003以内,表明Hf同位素数据质量较好。

流纹岩中大部分锆石分析点的 $^{176}\text{Lu}/^{177}\text{Hf}$ 比值小于0.002,表明锆石在形成以后有较少的放射成因Hf的累积^[32],获得的 $^{176}\text{Hf}/^{177}\text{Hf}$ 比值能够代表其形成时体系的Hf同位素组成^[33]。流纹岩锆石具有一致的 $^{176}\text{Hf}/^{177}\text{Hf}$ 初始比值,19个点的 $(^{176}\text{Hf}/^{177}\text{Hf})_i$ 比值变化于0.28276~0.28302, $\varepsilon_{\text{Hf}(t)}$ 值(322 Ma)介于6.3~15.5,平均值为12.6;所有锆石的 $f_{\text{Lu/Hf}}$ 变化于-0.93~-0.87,明显小于镁铁质地壳的 $f_{\text{Lu/Hf}}(-0.34)$ 和硅铝质地壳的 $f_{\text{Lu/Hf}}(-0.72)$ ^[34],因此其二阶段模式年龄(t_{DM2})(340~931 Ma)代表了源岩脱离亏损地幔的时间。

闪长玢岩10粒锆石分析点的 $^{176}\text{Lu}/^{177}\text{Hf}$ 比值小于0.002,它们可以代表闪长玢岩形成时的Hf同位素组成。这些分析的 $(^{176}\text{Hf}/^{177}\text{Hf})_i$ 比值变化于0.2821~0.2830, $\varepsilon_{\text{Hf}(t)}$ 值(322 Ma)变化较大,介于-0.22~13.9,说明有不同来源的物质的参与。单阶段Hf模式年龄(t_{DM})为401~954 Ma,二阶段模式年

龄(t_{DM2})为445~1347 Ma。

6 讨 论

东天山地区晚古生代岩浆活动剧烈,前人在东天山地区发现了大量石炭纪时期岩浆活动记录,如在大南湖—头苏泉带,李向民等^[35]获得了企鹅山群基性和酸性火山岩的锆石U-Pb年龄为(323±2)Ma和(320±2)Ma。侯广顺等^[36]获得了企鹅山群安山岩的SHRIMP锆石U-Pb年龄为(337±6)Ma。李源等^[37]利用LA-ICP-MS锆石U-Pb法,获得了哈盆地南缘底坎尔组流纹岩的年龄为(320±1.2)Ma。在阿奇山—雅满苏带内,吴昌志等^[38]获得了红云滩花岗岩锆石U-Pb年龄为328 Ma;苏春乾等^[39]获得了阿奇山组英安岩的SHRIMP锆石U-Pb年龄为(341.7±1.2)Ma;周涛发等^[40]利用LA-ICP-MS锆石U-Pb法,获得了百灵山花岗闪长岩年龄为(317.7±3.7)Ma,天目钾长花岗岩为(320.2±3.1)Ma。宋安江等^[41]获得了阿其克库都克断裂西段土古土布拉克组沉积砾石源岩的SHRIMP锆石U-Pb年龄为(314±4.2)Ma。关于底坎尔组和沙泉子铁铜矿床的形成时代,前人也做了大量的研究工作,如新疆维吾尔自治区地质矿产局在1958年根据底坎尔组地层中发现的腕足类、瓣类和珊瑚等化石,将其时代确定为中石炭世^[42]。冯京等^[42]、李永军等^[43]在库姆塔格沙垄北一带进行1:5万区调工作时,采集到了*Idiognathodus delicatus*、*Idiognathoides sinuata*、*Streptognathodus suberectus*、*S. meekerensis*、*S. exepansus*和*Streptognathodus sp.*(牙形刺),确定底坎尔组属晚石炭世。Huang et al.^[44]利用Re-Os法获得了沙泉子铁铜矿区磁铁矿和黄铁矿的形成年龄(300 Ma)。然而,对石炭纪时期所处的构造环境存在有岛弧^[37,42~43,45~50]、裂谷^[3,8,51,52]和地幔柱^[53]的争议,对古亚洲洋的俯冲方向有双向俯冲^[1,45,46,54],康古尔洋洋南向俯冲^[11,37,51]和北向俯冲的争议^[4],古亚洲洋闭合时间有早石炭世^[8,48]、中石炭世^[23]和晚石炭世^[55]的认识。

底坎尔组是一套火山岩—正常沉积岩和含丰富化石的灰岩组合,并且火山岩是以中基性火山岩为主体的钙碱性火山岩系列,显示了岛弧环境岩石组合特征。中基性火山岩具有亏损Nb、Ta、Ti等高场

强元素,富集大离子亲石元素和轻稀土元素的类似于岛弧火山岩的地球化学特征。并且流纹岩的Yb< 5×10^{-6} , Ta< 1×10^{-6} , Ta/Yb<0.5, Th>>Ta, 岩石的A/CNK均小于1.05等与俯冲作用有关的弧岩浆作用的特点^[56]。在Th-Ta-Hf/3图解中(图7-a),玄武岩位于岛弧环境玄武岩区。在不相容元素Yb标准化的Th-Nb二元协变图中,玄武岩位于大陆岛弧玄武岩和大洋岛弧玄武岩的重叠区,并且明显偏向大陆岛弧区域(图7-b,c)。中性岩的样品在Y-Sr/Y图解中均落入经典岛弧岩石区(7-d)。

玄武岩的Zr/Nb=41.8~48, Hf/Ta=16.9~23.6, 暗示其源区为类似于N-MORB的亏损地幔。(Th/Nb)_N(4.2~7.3)远大于1,(Nb/La)_N(0.21~0.24)和(La/Ba)_N(0.1~0.24)小于1,表明岩浆在演化过程中有地壳物质的混染。所有岩石富集大离子亲石元素和轻稀土元素,亏损Nb、Ta和Ti以及低的Ce/Pb(0.63~1.95)和Nb/U(1.2~3.1)比值,暗示源区有俯冲流体的加入,高的Ce/Th(15~22.7)和Ba/Th(>124)比值,并且缺乏Ce的负异常,低的TiO₂和Nb含量,表明源区没有俯冲沉积物熔体和俯冲板片熔体的加入。它们低的Mg[#]=0.60~0.65和Cr、Co、Ni值以及它们之间的正相关性,表明母岩浆经历了橄榄石和尖晶石的分离结晶过程。所有中性岩具有一致的元素地球化学特征,表明来自相同的源区。闪长玢岩中锆石的ε_{Hf(t)}值为变化大的正值,但低于亏损地幔的值,表明成岩过程中亏损的幔源岩浆中混有其他来源的物质。它们与玄武岩具有相似的元素地球化学特征,并且主量元素具有连续变化趋势,暗示了它们的亲缘性,中性岩应该是受板片流体强烈交代的地幔楔熔体分离结晶的产物。

流纹岩与基性和中性岩具有完全不同的元素地球化学特征,并具有高的ε_{Hf(t)}值,锆石的U-Pb年龄与Hf模式年龄接近(表3),在(176Hf/177Hf)_i-ε_{Hf(t)}与U-Pb年龄关系图中(图8),所有样品落入球粒陨石和亏损地幔之间接近球粒陨石演化线的上侧,说明岩浆来源于新生地壳物质的重熔。岩石具有高的Si含量、低的Cr及Ni的含量(分别为 1.65×10^{-6} ~ 4.25×10^{-6} 和 5.04×10^{-6} ~ 10.0×10^{-6}),表明岩浆体系没有受到地幔物质的混染。岩石具有明显的Eu负异常,强烈亏损Sr、Ba、P和Ti等元素,表明源区矿物相

^①新疆地矿局第一地质大队. K-46-66-D等8幅1:5万区域地质调查联测报告[R]. 1995.

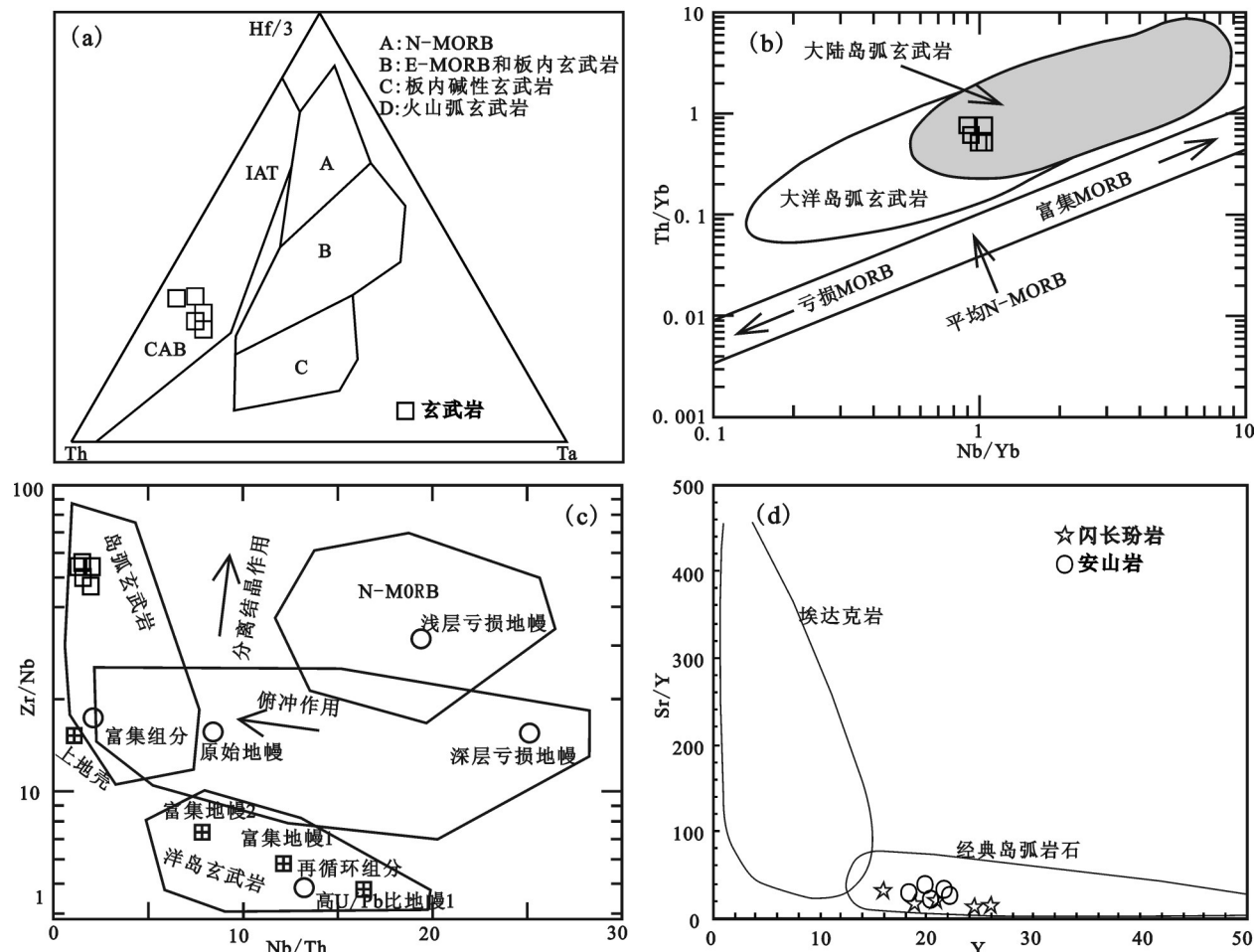


图7 沙泉子铁铜矿区火山岩构造环境判别图 (Sr/Y-Y底图据文献[57], Th-Ta-Hf/3底图据文献[58], Nb/Th-Zr/Nb底图据文献[59], Nb/Yb-Th/Yb底图据文献[60])

Fig.7 Discrimination diagram of tectonic setting of the volcanic rocks from the Shaquanzi Fe-Cu ore district, East Tianshan Mountains (Sr/Y-Y diagram after reference [57], Th-Ta-Hf/3 ternary discrimination diagram after reference [58], Nb/Th-Zr/Nb diagram after reference [59], Nb/Yb-Th/Yb diagram after reference [60])

中有斜长石、磷灰石、角闪石、钛铁矿残留^[61],岩石中见有碱性长石、钠长石和黑云母斑晶,表明可能发生了弱的结晶分异作用。

上述分析表明,底坎尔组火山岩和闪长玢岩应该是早石炭世末大陆岛弧环境的产物,这与前人对区域上早石炭世雅满苏组和阿奇山组火山岩是成熟岛弧环境产物^[37,66,67]的认识一致。也表明古天山洋在晚石炭世尚未闭合。同时,它们与新疆北部阿尔泰地区含矿火山岩的形成环境和物质来源特征一致^[68]。由俯冲板片流体交代的地幔楔部分熔融形成的玄武质岩浆携带 Fe_2O_3 、 H_2O 和 Cl 等大量挥发分,由于挥发分的存在增加 Fe 在岩浆中的溶解度,并且 Cl 在高温高压下是携带 Fe^{3+} 等金属离子的有效

络合剂,可以与 Fe 形成络合物运移^[69],在有利部位聚集形成矿床。至于这些富含挥发分和 Fe_2O_3 的岩浆是通过液态不混溶作用还是流体出溶作用形成的铁矿床,具体过程还有待进一步研究。

本研究利用LA-ICP-MS锆石U-Pb法获得了流纹岩(321.7 ± 1.7)Ma和闪长玢岩(322.2 ± 1.7)Ma的年龄结果,均是通过震荡环带发育的岩浆锆石测得的,并且谐和性较好,可以代表锆石结晶年龄。尽管闪长玢岩侵入底坎尔组火山岩地层,两个年龄在误差范围内近于一致,可以接受。因此,这些年龄可以代表沙泉子铁铜矿区底坎尔组流纹岩的喷发年龄和闪长玢岩的侵位年龄,即底坎尔组火山岩和闪长玢岩是早石炭世末岩浆活动的产物。沙泉子铁铜矿体赋存于火

表3 沙泉子矿区流纹岩和闪长玢岩中锆石原位Hf同位素分析数据

Table 3 Zircon Hf composition of the rhyolite and diorite–porphyrite in the Shaquanzi Fe–Cu ore district, East Tianshan Mountains

点号	$^{176}\text{Yb}/^{177}\text{Hf}$	$^{176}\text{Lu}/^{177}\text{Hf}$	$^{176}\text{Hf}/^{177}\text{Hf}$	2σ	$^{176}\text{Hf}/^{177}\text{Hf}_{\text{t}}$	$\varepsilon_{\text{Hf}(0)}$	t_{DM}	t_{DM2}
样品编号: sqz78								
sqz 78.1	0.2477	0.0057	0.282857	0.000030	0.28282	8.8	641	768
sqz 78.2	0.0694	0.0016	0.283020	0.000020	0.28301	15.5	333	340
sqz 78.3	0.1240	0.0029	0.282827	0.000025	0.28281	8.4	635	797
sqz 78.4	0.0846	0.0021	0.282846	0.000020	0.28283	9.2	593	743
sqz 78.5	0.1240	0.0026	0.282872	0.000021	0.28286	10.1	562	690
sqz 78.6	0.0569	0.0016	0.282760	0.000018	0.28275	6.3	709	931
sqz 78.8	0.0579	0.0014	0.282974	0.000017	0.28297	13.9	398	443
sqz 78.11	0.0571	0.0014	0.282943	0.000018	0.28294	12.8	442	512
sqz 78.13	0.0502	0.0014	0.282942	0.000017	0.28293	12.8	444	515
sqz 78.15	0.0391	0.0010	0.282933	0.000017	0.28293	12.5	453	532
sqz 78.16	0.0629	0.0018	0.283002	0.000016	0.28299	14.9	361	385
sqz 78.17	0.0733	0.0021	0.282927	0.000020	0.28291	12.3	475	561
sqz 78.18	0.0539	0.0016	0.282943	0.000022	0.28293	12.9	444	515
sqz 78.19	0.0458	0.0014	0.282956	0.000014	0.28295	13.3	423	482
sqz 78.20	0.0551	0.0016	0.282978	0.000017	0.28297	14.0	395	437
sqz 78.22	0.0513	0.0015	0.282967	0.000015	0.28296	13.6	409	460
sqz 78.23	0.0635	0.0018	0.283019	0.000017	0.28301	15.4	337	346
sqz 78.25	0.0434	0.0013	0.282965	0.000019	0.28296	13.7	409	461
sqz 78.26	0.0541	0.0015	0.282962	0.000016	0.28295	13.5	416	471
sqz 78.27	0.0532	0.0015	0.282975	0.000019	0.28297	13.9	398	442
sqz 78.28	0.0564	0.0015	0.283016	0.000018	0.28301	15.4	339	349
sqz 78.30	0.0573	0.0015	0.283000	0.000018	0.28299	14.9	362	386
样品编号: sqz99								
sqz 99.2	0.0615	0.0016	0.282887	0.000019	0.28288	10.8	527	643
sqz 99.3	0.0884	0.0023	0.282913	0.000018	0.2829	11.6	497	591
sqz 99.6	0.0359	0.0011	0.282587	0.000016	0.28258	0.332	944	1312
sqz 99.7	0.0891	0.0029	0.282982	0.000020	0.28296	13.9	403	445
sqz 99.8	0.1245	0.0043	0.282970	0.000029	0.28294	13.2	439	491
sqz 99.10	0.1390	0.0047	0.282924	0.000028	0.2829	11.5	516	600
sqz 99.12	0.0754	0.0026	0.282826	0.000021	0.28281	8.5	631	794
sqz 99.14	0.0801	0.0025	0.282833	0.000019	0.28282	8.8	618	775
sqz 99.15	0.0546	0.0020	0.282662	0.000019	0.28265	2.8	859	1156
sqz 99.16	0.0695	0.0022	0.282661	0.000018	0.28265	2.7	864	1160
sqz 99.17	0.0647	0.0017	0.282868	0.000019	0.28286	10.1	555	687
sqz 99.19	0.2015	0.0065	0.282902	0.000045	0.28286	10.3	582	676
sqz 99.20	0.0877	0.0019	0.282938	0.000022	0.28293	12.6	456	530
sqz 99.21	0.0714	0.0019	0.282576	0.000019	0.28256	-0.22	980	1347
sqz 99.23	0.1278	0.0036	0.282930	0.000027	0.28291	11.9	490	570
sqz 99.24	0.0812	0.0019	0.282975	0.000020	0.28296	13.9	401	445
sqz 99.28	0.0839	0.0021	0.282943	0.000020	0.28293	12.7	451	522
sqz 99.30	0.1009	0.0031	0.282900	0.000034	0.28288	10.9	530	634

注:Hf同位素分析采用标准球粒陨石($^{176}\text{Lu}/^{177}\text{Hf}$)_{CHUR}=0.32, ($^{176}\text{Hf}/^{177}\text{Hf}$)_{CHUR,0}=0.282772^[63]; 亏损地幔($^{176}\text{Lu}/^{177}\text{Hf}$)_{DM}=0.0384, ($^{176}\text{Hf}/^{177}\text{Hf}$)_{DM}=0.28325^[64]; Lu衰变常数 $\lambda=1.867\times 10^{-11}\text{a}^{[65]}$ 。

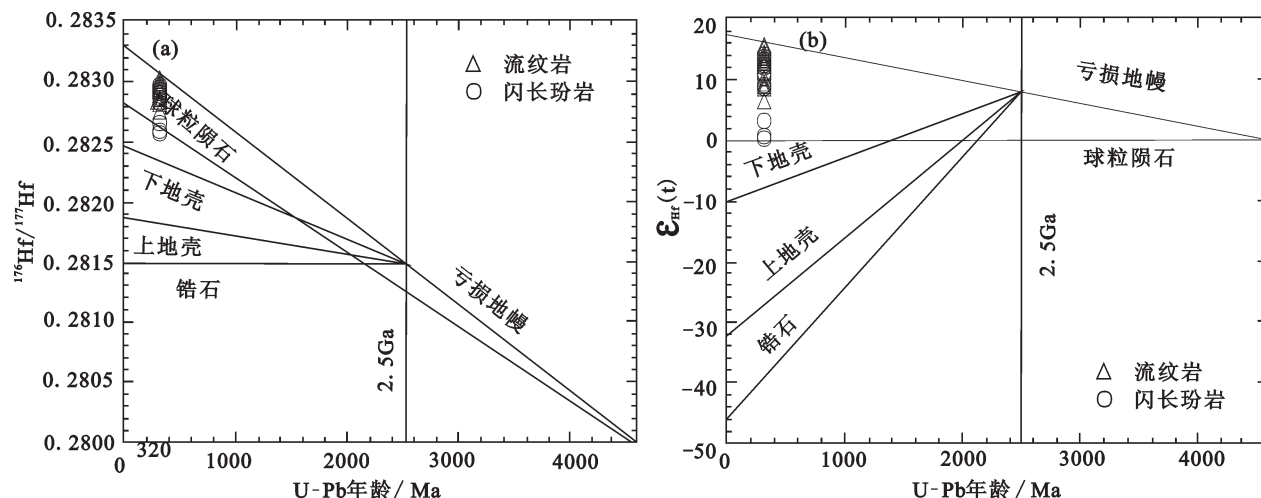


图8 沙泉子流纹岩及闪长玢岩的单阶段模式年龄计算示意图(a)及与年龄相关图(b) (据资料[62]修改)

Fig.8 Single-stage Hf model age calculation (a) and correlation diagram of zircon ε_{Hf} versus U-Pb (b) age of the rhyolite and diorite-porphyrite in the Shaquanzi Fe-Cu ore district, East Tianshan Mountains (after reference [62])

山岩中，并呈层状、似层状及透镜状顺层分布，在闪长玢岩与围岩接触带发育铁矿化，该铁矿化与火山作用有关，其形成不早于322 Ma。

7 结 论

沙泉子铁铜矿区底坎尔组火山岩为基性-中性-酸性连续序列，以中基性岩为主。火山岩主要属钙碱性系列，富集轻稀土元素(LREE)和大离子亲石元素(LILE)，亏损高场强元素(Nb、Ta、Ti)，整体表现出大陆岛弧火山岩的地球化学特征。LA-ICP-MS锆石U-Pb获得流纹岩和闪长玢岩的形成时代非常接近， $^{206}\text{Pb}/^{238}\text{U}$ 加权平均年龄分别为 $(321.7 \pm 1.70)\text{ Ma}$ 和 $(322.2 \pm 1.70)\text{ Ma}$ 。基性、中性和酸性岩来自不同的源区。综合区域地质资料，矿区火山岩可能属俯冲相对晚期阶段大陆岛弧岩浆作用的产物。铁矿化不早于322 Ma，幔源岩浆为铁矿化提供了重要的物质来源。

致谢：野外期间得到新疆地质矿产勘探开发局第六地质大队的支持。样品的年龄测试得到了中国地质科学院矿产资源研究所侯可军老师、郭春丽老师的帮助。样品的主要元素、微量及稀土元素由广州澳石分析测试中心完成，在此一并表示感谢。

参考文献(References):

[1] 姬金生, 陶洪祥, 曾章仁, 等. 东天山康古尔塔格金矿带地质与成

矿[M]. 北京: 地质出版社, 1994: 1–200.

Ji Jinsheng, Tao Hongxiang, Zeng Zhangren, et al. Geology and Exploration of Gold Deposit in Kanggu’ Ertage Belt, Eastern Tianshan[M]. Beijing: Geological Publishing House, 1994: 1–200 (in Chinese with English Abstract).

[2] 秦克章, 方同辉, 王书来. 东天山板块构造分区、演化与成矿地质背景研究[J]. 新疆地质, 2002, 20(4): 302–308.

Qin Kezhang, Fang Tonghui, Wang Shulai. Plate tectonics division, evolution and metallogenic settings in eastern Tianshan mountains, NW-China[J]. Xinjiang Geology, 2002, 20(4): 302–308 (in Chinese with English Abstract).

[3] 秦克章, 彭晓明, 三金柱, 等. 东天山主要矿床类型、成矿区带划分与成矿远景区优选[J]. 新疆地质, 2003, 21(2): 143–150.

Qin Kezhang, Peng Xiaoming, San Jinzhu, et al. Types of major ore deposits, division of metallogenic belts in Eastern Tianshan, and discrimination of potential prospects of Cu, Au, Ni mineralization[J]. Xinjiang Geology, 2003, 21(2): 143–150 (in Chinese with English Abstract).

[4] Xiao Wenjiao, Zhang Lianchang, Qin Kezhang, et al. Paleozoic accretionary and collisional tectonics of the eastern Tianshan (China): implications for the continental growth of Central Asia[J]. American Journal of Science, 2004, 304: 370–395.

[5] 王京彬, 王玉往, 何志军. 东天山大地构造演化的成矿示踪[J]. 中国地质, 2006, 33: 461–469.

Wang Jingbin, Wang Yuwang, He Zhijun. Ore deposits as a guide to the tectonic evolution in the East Tianshan Mountains, NW China [J]. Geology in China, 2006, 33: 461–469 (in Chinese with English Abstract).

[6] 张连昌, 夏斌, 牛贺才, 等. 新疆晚古生代大陆边缘成矿系统与成矿区带初步探讨[J]. 岩石学报, 2006, 5: 1387–1398.

- Zhang Lianchang, Xia Bin, Niu Hecai, et al. Metallogenic systems and belts developed on the late Paleozoic continental margin in Xinjiang[J]. *Acta Petrologica Sinica*, 2006, 22(5): 1387–1398 (in Chinese with English Abstract).
- [7] 顾连兴, 胡受奚, 于春水, 等. 东天山博格达造山带石炭纪火山岩及其形成地质环境[J]. *岩石学报*, 2000, 16(3): 305–316.
- Gu Lianxing, Hu Shouxi, Yu Chunshui, et al. Carboniferous volcanites in the Bogda orogenic belt of eastern Tianshan: Their tectonic implications[J]. *Acta Petrologica Sinica*, 2000, 16(3): 305–316 (in Chinese with English abstract).
- [8] 夏林圻, 张国伟, 夏祖春, 等. 天山古生代洋盆开启、闭合时限的岩石学约束——来自震旦纪、石炭纪火山岩的证据[J]. *地质通报*, 2002, 21(2): 55–62.
- Xia Linqi, Zhang Guowei, Xia Zuchun, et al. Constraints on the timing of opening and closing of the Tianshan Paleozoic oceanic basin: Evidence from Sinian and Carboniferous volcanic rocks[J]. *Geological Bulletin of China*, 2002, 21(2): 55–62 (in Chinese with English abstract).
- [9] 马瑞士, 舒良树, 孙家齐. 东天山构造演化与成矿[M]. 北京: 科学出版社, 1997: 152–170.
- Ma Ruishi, Shu Liangshu, Sun Jiaqi. *Tectonic Evolution and Metallization of Eastern Tianshan*[M]. Beijing: Science Press, 1997: 152–170 (in Chinese with English abstract).
- [10] 李锦轶, 王克卓, 李文铅, 等. 东天山晚古生代以来大地构造与矿产勘查[J]. *新疆地质*, 2002, 22(4): 295–301.
- Li Jinzhi, Wang Kezhuo, Li Wenqian, et al. Tectonic evolution since the late Paleozoic and mineral prospecting in eastern Tianshan Mountains, NW China[J]. *Xinjiang Geology*, 2002, 22(4): 295–301 (in Chinese with English Abstract).
- [11] 左国朝, 梁广林, 陈俊, 等. 东天山觉罗塔格地区夹白山一带晚古生代构造格局及演化[J]. *地质通报*, 2006, 25(1/2): 48–57.
- Zuo Guochao, Liang Guanglin, Chen Jun, et al. Late Paleozoic tectonic framework and evolution in the Jiabaishan area, Qoltag, Eastern Tianshan mountains, NW China[J]. *Geological Bulletin of China*, 2006, 25(1/2): 48–57 (in Chinese with English abstract).
- [12] Zhang Z C, Hou T, M. Santosh, et al. Spatio-temporal distribution and tectonic settings of the major iron deposits in China: An overview[J]. *Ore Geology Reviews*, 54: 247–263.
- [13] 宋治杰, 魏士娥. 新疆库姆塔格—沙泉子一带早—中石炭世的火山岩系[J]. 中国地质科学院西安地质矿产研究所所刊, 1982, (4): 76–93.
- Song Zhijie, Wei Shie. The early and middle Carboniferous volcanic rock series of Kumtag– Shaquanzi zone, Xinjiang[J]. *Bull.Xi'an Inst.Geo1. Min. Res., Chinese Acad. Geo1. Sci.*, 1982, (4): 76–93 (in Chinese with English abstract).
- [14] 宋治杰. 新疆哈密火山—侵入杂岩地区一组磁铁矿床的形成条件与成矿作用[J]. 中国地质科学院西安地质矿产研究所所刊, 1985, (9): 58–73.
- Song Zhijie. The formative conditions and mineralization of a group of magnetite in volcanic– intrusive complex region near Hami, Xinjiang[J]. *Bull. Xi'an Inst. Geo1. Min. Res., Chinese Acad. Geo1.Sci.*, 1985, (9): 58–73 (in Chinese with English abstract).
- [15] 何大伦, 周济元, 茅燕石. 东天山火山型铁矿床的产出特征及成矿机制[J]. 新疆地质科学第五辑, 1994: 41–53.
- He Dalun, Zhou Jiyuan, Mao Yanshi. Output characteristics and metallogenic mechanism of volcanic type iron deposits, eastern Tianshan[J]. *Xinjiang Fifth Series of Geological Sciences*, 1994: 41–53 (in Chinese with English Abstract).
- [16] 冯京, 徐仕琪, 田江涛, 等. 东天山海相火山岩型铁矿成矿规律研究方法[J]. *新疆地质*, 2009, 27(4): 330–336.
- Feng Jing, Xu Shiqi, Tian Jiangtao, et al. Study on metallogenic regularity of marine volcanic type iron ore of East Tianshan of Xinjiang and methods discuss[J]. *Xinjiang Geology*, 2009, 27(4): 330–336 (in Chinese with English Abstract).
- [17] 张洪武, 谢丽霞. 对雅满苏铁矿床成因的新认识[J]. *长春工程学院学报(自然科学版)*, 2001, 2(4): 26–29.
- Zhang Hongwu, Xie Lixia. New views on origin of Yamansu iron deposit in Xinjiang Autonomous Region[J]. *Changchun Inst. Tech. (Nar. Sci. Edi.)*, 2001, 2(4): 26–29 (in Chinese with English Abstract).
- [18] 姜福芝, 秦克章, 方同辉, 等. 东天山铁矿床类型、地质特征成矿规律与找矿方向[J]. *新疆地质*, 2002, 20(4): 379–383.
- Jiang Fuzhi, Qin Kezhang, Fang Tonghui, et al. Types, geological characteristics, metallogenic regulaiuty and exploration target of iron deposits in eastern Tianshan Mountains[J]. *Xinjiang Geology*, 2002, 20(4): 379–383 (in Chinese with English abstract).
- [19] 徐晓彤, 袁万明, 龚庆杰, 等. 利用裂变径迹定年分析新疆沙泉子铜铁矿成矿时代[J]. *中国矿业*, 2010, 19(4): 105–108.
- Xu Xiaotong, Yuan Wanming, Gong Qingjie, et al. The analysis of zircon fission track's ore-forming epoch in Shaquanzi copper–iron deposits, Xinjiang[J]. *China Mining Magazine*, 2010, 19(4): 105–108 (in Chinese with English Abstract).
- [20] 黄小文, 漆亮, 孟郁苗. 东天山黑峰山、双峰山及沙泉子(铜)铁矿床的矿物微量和稀土元素地球化学特征[J]. *矿床地质*, 2013, 32(6): 1188–1210.
- Huang Xiaowen, Qi Liang, Meng Yumiao. Trace element and REE geochemistry of minerals from Heifengshan, Shuangfengshan and Shaquanzi (Cu–) Fe Deposits, Eastern Tianshan Mountains[J]. *Mineral Deposits*, 2013, 32(6): 1188–1210 (in Chinese with English abstract).
- [21] 黄小文, 漆亮, 王怡昌, 等. 东天山沙泉子铜铁矿床磁铁Re–Os定年初探[J]. *中国科学(D辑)*, 2014, 44(4): 605–616.
- Huang Xiaowen, Qi Liang, Wang Yichang, et al. Preliminary dating magnetite Re– Os of Shaquanzi Fe(– Cu) deposits, Eastern Tianshan[J]. *Science in China (Series D)*, 2014, 44(4): 605–616 (in Chinese).
- [22] 黄小文, 漆亮, 高剑峰, 等. 东天山觉罗塔格地区底坎儿组火山

- 岩地球化学特征及构造环境探讨[J]. 岩石矿物学杂志, 2012, 31(6): 799–817.
- Huang Xiaowen, Qi Liang, Gao Jianfeng, et al. Geochemistry of volcanic rocks in the Dikan'er Formation of Jueluotage region, eastern Tianshan Mountains and its tectonic implications[J]. *Acta Petrologica et Mineralogica*, 2012, 31(6): 799–817 (in Chinese with English abstract).
- [23] 李文明, 任秉琛, 杨兴科, 等. 东天山中酸性侵入岩浆作用及其地球动力学意义[J]. 西北地质, 2002, 35(4): 41–64.
- Li Wenming, Ren Bingchen, Yang Xingke, et al. The intermediate-acid intrusive magmatism and its geodynamic significance in Eastern Tianshan region[J]. *Northwestern Geology*, 2002, 35(4): 41–64 (in Chinese with English abstract).
- [24] Su B X, Qin K Z, Sakyi Patrick Asamoah, et al. Geochemistry and geochronology of acidic rocks in the Beishan region, NW China: Petrogenesis and tectonic implications[J]. *Journal of Asia Earth Science*, 2011, 41: 31–43.
- [25] Winchester J A, Floyd P A. Geochemical discrimination of different magma series and their differentiation products using immobile elements[J]. *Chemical Geology*, 1977, 80: 325–343.
- [26] Sun S S, McDonough W F. Chemical and isotopic systematics of oceanic basalts: implications for mantle composition and processes[C]//Saunders A D, Norry M J (eds.). *Magmatism in the Ocean Basins*. Geological Society Special Publication, 1989, 42: 313–345.
- [27] 侯可军, 李延河, 田有荣. LA-MC-ICP-MS锆石微区原位U-Pb定年技术[J]. 矿床地质, 2009, 28(4): 481–492.
- Hou Kejun, Li Yanhe, Tian Yourong. Insitu U-Pb zircon dating using laser ablation-multion cutting-ICP-MS[J]. *Mineral Deposits*, 2009, 28(4): 481–492 (in Chinese with English abstract).
- [28] Liu Y S, Hu Z C, Gao S, et al. In situ analysis of major and trace elements of anhydrous minerals by LA-ICP-MS without applying an internal standard[J]. *Chemical Geology*, 2008, 257: 34–43.
- [29] Ludwig K R. Using Isoplot/Ex, version 2.49[C]//A geochronological toolkit for Microsoft Excel. Berkeley Geochronological Center Special Publication, Berkeley, 2001: 1–55.
- [30] Rubatto D. Zircon trace element geochemistry: Partitioning with garnet and the link between U-Pb ages and metamorphism[J]. *Chemical Geology*, 2002, 184: 123–138.
- [31] 李怀坤, 朱士兴, 相振群, 等. 北京延庆高于庄组凝灰岩的锆石U-Pb定年研究及其对华北北部中元古界划分新方案的进一步约束[J]. 岩石学报, 2010, 26(7): 2131–2140.
- Li Huaikun, Zhu Shixing, Xiang Zhenqun, et al. Zircon U-Pb dating on tuf fbed from Gaoyuzhuang Formation in Yanqing, Beijing: Further constraints on the new subdivision of the Mesoproterozoic stratigraphy in the northern North China Craton[J]. *Acta Petrologica Sinica*, 26(7): 2131–2140 (in Chinese with English abstract).
- [32] 杨进辉, 吴福元, 邵济安, 等. 冀北张宣地区后城组、张家口组火山岩锆石U-Pb年龄和Hf同位素[J]. 地球科学, 2006, 31(1): 71–80.
- Yang Jinhuai, Wu Fuyuan, Shao Ji'an. In-Situ U-Pb dating and Hf isotopic analyses of zircons from volcanic rocks of the Houcheng and Zhangjiakou Formations in the Zhang-Xuan area, northeast China[J]. *Earth Science*, 2006, 31(1): 71–80 (in Chinese with English Abstract).
- [33] 吴福元, 李献华, 郑永飞, 等. Lu-Hf同位素体系及其岩石学应用[J]. 岩石学报, 2007, 23(2): 185–220.
- Wu Fuyuan, Li Xianhua, Zheng Yongfei, et al. Lu-Hf isotope systematics and their applications in petrology[J]. *Acta Petrologica Sinica*, 2007, 23(2): 185–220 (in Chinese with English abstract).
- [34] Vervoort J D, Pachelt P J, Gehrels G E, et al. Constraints on earth Earth differentiation from hafnium and neodymium isotopes[J]. *Nature*, 1996, 397 (6566): 624–627.
- [35] 李向民, 夏林圻, 夏祖春, 等. 东天山企鹅山群火山岩锆石U-Pb年代学[J]. 地质通报, 2004, 23(12): 1215–1220.
- Li Xiangmin, Xia Linqi, Xia Zuchun, et al. Zircon U-Pb geochronology of volcanic rocks of the Qi'eshan Group in the East Tianshan Mountains[J]. *Geological Bulletin of China*, 2004, 23(12): 1215–1220 (in Chinese with English abstract).
- [36] 侯广顺, 唐红峰, 刘丛强, 等. 东天山土屋-延东斑岩铜矿围岩的同位素年代和地球化学研究[J]. 岩石学报, 2005, 21(6): 1729–1736.
- Hou Guangshun, Tang Hongfeng, Liu Conqiang, et al. Geochronological and geochemical study on the wallrock of Tuwu-Yandong porphyry copper deposits, eastern Tianshan mountains[J]. *Acta Petrologica Sinica*, 2005, 21(6): 1729–1736 (in Chinese with English Abstract).
- [37] 李源, 杨经绥, 张健, 等. 新疆东天山石炭纪火山岩及其构造意义[J]. 岩石学报, 2011, 27(1): 193–209.
- Li Yuan, Yang Jingsui, Zhang Jian, et al. Tectonical significance of the Carboniferous volcanic rocks in eastern Tianshan[J]. *Acta Petrologica Sinica*, 2011, 27(1): 193–209 (in Chinese with English abstract).
- [38] 吴昌志, 张遵忠, Khin Zaw, 等. 东天山觉罗塔格红云滩花岗岩年代学、地球化学及其构造意义[J]. 岩石学报, 2006, 22(5): 1121–1134.
- Wu Changzhi, Zhang Zunzhong, Zaw K, et al. Geochronology, geochemistry and tectonic significances of the Hongyuntan granitoids in the Qoltag area, Eastern Tianshan[J]. *Acta Petrologica Sinica*, 2006, 22(5): 1121–1134 (in Chinese with English abstract).
- [39] 苏春乾, 姜常义, 夏明哲, 等. 北天山东段阿奇山组火山岩的地球化学特征及锆石U-Pb年龄[J]. 岩石学报, 2009, 25(4): 901–915.
- Su Chunqian, Jiang Changyi, Xia Mingzhe, et al. Geochemistry

- and zircons SHRIMP U-Pb age of volcanic rocks of Aqishan Formation in the eastern area of north Tianshan, China[J]. *Acta Petrologica Sinica*, 2009, 25(4): 901–915 (in Chinese with English abstract).
- [40] 周涛发, 袁峰, 张达玉, 等. 新疆东天山觉罗塔格地区花岗岩类年代学、构造背景及其成矿作用研究[J]. *岩石学报*, 2010, 26(2): 478–502.
- Zhou Taofa, Yuan Feng, Zhang Dayu, et al. Geochronology, tectonic setting and mineralization of granitoids in Jueluotage area, eastern Tianshan, Xinjiang[J]. *Acta Petrologica Sinica*, 2010, 26(2): 478–502 (in Chinese with English abstract).
- [41] 宋安江, 朱志新, 石莹, 等. 东天山阿其克库都克断裂西段土古土布拉克组锆石 SHRIMP U-Pb 测年[J]. *地质通报*, 2006, 25(8): 953–956.
- Song Anjiang, Zhu Zhixin, Shi Ying, et al. SHRIMP U-Pb dating of zircons from the Tugutu Bulak Formation in the western segment of the Aqqikkuduk fault in the East Tianshan, Xinjiang, China[J]. *Geological Bulletin of China*, 2006, 25(8): 953–956 (in Chinese with English abstract).
- [42] 冯京, 李永军, 王晓刚, 等. 东天山库姆塔格沙垄地区石炭纪化石新资料及地层厘定[J]. *中国地质*, 2007, 34(5): 942–949.
- Feng Jing, Li Yongjun, Wang Xiaogang, et al. Redefinition of Carboniferous lithostratigraphic units in the Kumtag sand-ridge area, East Tianshan, based on new fossil evidence[J]. *Geology in China*, 2007, 34(5): 942–949 (in Chinese with English abstract).
- [43] 李永军, 刘晓宇, 王晓刚, 等. 东天山库姆塔格石炭纪牙形石的发现及地质意义[J]. *新疆地质*, 2007, 25(2): 127–131.
- Li Yongjun, Liu Xiaoyu, Wang Xiaogang, et al. The discovery of fossils in carboniferous of Kumutag area in the eastern Tianshan and its significance[J]. *Xingiang Geology*, 2007, 25(2): 127–131 (in Chinese with English abstract).
- [44] Huang X W, Qi L, Gao J F, et al. First reliable Re-Os ages of pyrite and stable isotope compositions of Fe(-Cu) deposits in the Hami region, Eastern Tianshan Orogenic Belt, NW China[J]. *Resource Geology*, 2013, 63(2): 166–187.
- [45] 李锦轶, 王克卓, 李文铅, 等. 东天山晚古生代以来大地构造与矿产勘查[J]. *新疆地质*, 2002, 22(4): 295–301.
- Li Jinyi, Wang Kezhuo, Li Wenqian, et al. Tectonic evolution since the late Paleozoic and mineral prospecting in Eastern Tianshan mountains, NW China[J]. *Xinjiang Geology*, 2002, 22(4): 295–301 (in Chinese with English abstract).
- [46] 侯广顺, 唐红峰, 刘丛强. 东天山觉罗塔格构造带晚古生代火山岩地球化学特征及意义[J]. *岩石学报*, 2006, 22(5): 1167–1177.
- Hou Guangshun, Tang Hongfeng, Liu Conqiang. Geochemistry characteristics of the Late Paleozoic volcanics in Jueluotage tectonic belt, eastern Tianshan and its implications [J]. *Acta Petrologica Sinica*, 2006, 22(5): 1167–1177 (in Chinese with English abstract).
- [47] 万博, 张连昌, 徐兴旺, 等. 东天山小石头泉铜多金属矿区火山岩-次火山岩地球化学与成矿构造背景[J]. *岩石学报*, 2006, 22(11): 2711–2718.
- Wan Bo, Zhang Lianchang, Xu Xingwang, et al. Geochemical characteristics of volcanic, sub-volcanic rocks in Xiaoshitouquan copper polymetallic deposit, eastern Tianshan, and its metallogenetic setting[J]. *Acta Petrologica Sinica*, 2006, 22(11): 2711–2718 (in Chinese with English abstract).
- [48] 王强, 赵振华, 许继峰, 等. 天山北部石炭纪埃达克岩-高镁安山岩-富Nb岛弧玄武质岩: 对中亚造山带显生宙地壳增生与铜金成矿的意义[J]. *岩石学报*, 2006, 21(1): 11–30.
- Wang Qiang, Zhao Zhenhua, Xu Jifeng, et al. Carboniferous adakite-high-Mg andesite-Nb-enriched basaltic rocks in the Northern Tianshan area: Implications for Phanerozoic crust growth in the Central Asia Orogenic Belt and Cu-Au mineralization[J]. *Acta Petrologica Sinica*, 2006, 21(1): 11–30 (in Chinese with English abstract).
- [49] 方维萱, 高珍权, 贾润幸, 等. 东疆沙泉子铜和铜铁矿床岩(矿)石地球化学研究与地质找矿前景[J]. *岩石学报*, 2006, 22(5): 1413–1424.
- Fang Weixuan, Gao Zhenquan, Jia Runxing, et al. Geological exploration potentials and geochemical study on rocks and ores in Shaquanzi copper and copper-iron deposits, east Xinjiang[J]. *Acta Petrologica Sinica*, 2006, 22(5): 1413–1424 (in Chinese with English abstract).
- [50] 朱永峰, 王涛, 徐新. 新疆及邻区地质与矿产研究进展[J]. *岩石学报*, 2007, 23(8): 1785–1794.
- Zhu Yongfeng, Wang Tao, Xu Xin. Progress of geology study in Xinjiang and its adjacent regions[J]. *Acta Petrologica Sinica*, 2007, 23(8): 1785–1794 (in Chinese with English abstract).
- [51] 顾连兴, 胡受奚, 于春水, 等. 论博格达俯冲撕裂型裂谷的形成与演化[J]. *岩石学报*, 2001, 17(4): 585–597.
- Gui Lianxing, Hu Shouxie, Yu Chunshui, et al. Initiation and evolution of the Bogda subduction-torn-type rift[J]. *Acta Petrologica Sinica*, 2001, 17(4): 585–597 (in Chinese with English abstract).
- [52] 陈丹玲, 刘良, 车自成, 等. 中天山骆驼沟火山岩的地球化学特征及其构造环境[J]. *岩石学报*, 2001, 17(3): 378–384.
- Chen Danling, Liu Liang, Che Zicheng, et al. Geochemical characteristics and tectonic implication of Carboniferous volcanites in the Luotuogou area of Middle Tianshan[J]. *Acta Petrologica Sinica*, 2001, 17(3): 378–384 (in Chinese with English abstract).
- [53] 夏林圻, 夏祖春, 徐学义, 等. 天山石炭纪大火成岩省与地幔柱[J]. *地质通报*, 2004, 23(9/10): 903–910.
- Xia Linqi, Xia Zuchun, Xu Xueyi, et al. Carboniferous Tianshan igneous megaprovince and mantle plume[J]. *Geological Bulletin of China*, 2004, 23(9/10): 903–910 (in Chinese with English abstract).
- [54] 周济元, 茅燕石, 黄志勋, 等. 东天山古大陆边缘火山地质[M]. 成都: 成都科技大学出版社, 1994: 1–200.

- Zhou Jiyuan, Mao Yanshi, Huang Zhixun, et al. Volcanology of East Tianshan Continental Margin[M]. Chengdu: Publishing House of Chengdu Sci. and Tech. University, 1994: 1–200 (in Chinese).
- [55] 张洪瑞, 魏刚峰, 李永军, 等. 东天山大南湖岛弧带石炭纪岩石地层与构造演化[J]. 岩石矿物学杂志, 2010, 29(1): 1–13.
- Zhang Hongrui, Wei Gangfeng, Li Yongjun, et al. Carboniferous lithologic association and tectonic evolution of Dananhu arc in the East Tianshan Mountains[J]. *Acta Petrologica et Mineralogica*, 2010, 29(1): 1–13 (in Chinese with English abstract).
- [56] Condie K C. Geochemistry and tectonic setting of Early Proterozoic supracrustal rocks in the southwestern United States[J]. *The Journal of Geology*, 1986, 94(6): 845–864.
- [57] Defant M J, Drummond M S. Derivation of some modern arc magmas by melting of young subducted lithosphere[J]. *Nature*, 1990, 347: 662–665.
- [58] Wood D A. The application of a Th–Hf–Ta diagram to problems of tectonomagmatic classification and to establishing the nature of crustal contamination of basaltic lavas of the British Tertiary Volcanic Province[J]. *Earth and Planetary Science Letters*, 1980, 50(1): 11–30.
- [59] Condie K C. High field strength element ratios in Archean basalts: A window to evolving sources of mantle plumes?[J]. *Lithos*, 2005, 79(3/4): 491–504.
- [60] Pearce J A, Peate D W. Tectonic implications of the composition of volcanic arc lavas[J]. *Annual Review of Earth and Planetary Sciences*, 1995, 23: 251–285.
- [61] Lighfoot P C, Hawkesworth C J, Sethna S F. Petrogenesis of rhyolites and trachytes from the Deccan Trap: Sr, Nd and Pb isotope and trace element evidence[J]. *Contributions to Mineralogy and Petrology*, 1987, 95(1): 44–54.
- [62] 唐冬梅, 秦克章, 孙赫, 等. 天宇铜镍矿床的岩相学、锆石U-Pb年代学、地球化学: 对东疆镁铁-超镁铁质岩体源区和成因的制约[J]. 岩石学报, 2009, 25(4): 817–831.
- Tang Dongmei, Qin Kezhang, Sun He, et al. Lithological, chronological and geochemical characteristics of Tianyu Cu–Ni deposit: Constraints on source and genesis in eastern Xinjiang[J]. *Acta Petrologica Sinica*, 2009, 25(4): 817–831 (in Chinese with English abstract).
- Zhou Jiyuan, Mao Yanshi, Huang Zhixun, et al. Volcanology of East Tianshan Continental Margin[M]. Chengdu: Publishing House of Chengdu Sci. and Tech. University, 1994: 1–200 (in Chinese).
- [63] Blichert-Toft J, Albarède F. The Lu–Hf isotope geochemistry of chondrites and the evolution of the mantle–crust system[J]. *Earth and Planetary Science Letters*, 1997, 148(1/2): 243–258.
- [64] Griffin W L, Pearson N J, Belousova E, et al. The Hf isotope composition of cratonic mantle: LA–MC–IC–PMS analysis of zircons megacrysts in kimberlites[J]. *Geochimica et Cosmochimica Acta*, 2000, 64(1): 133–147.
- [65] Söderlund U, Patchett P J, Vervoort J D, et al. The ^{176}Lu decay constant determined by Lu–Hf and U–Pb isotope systematics of Precambrian mafic intrusions[J]. *Earth and Planetary Science Letters*, 2004, 219(3/4): 311–324.
- [66] 阎文元. 天山东段早中石炭世岛弧型火山岩特征及其矿产[J]. 新疆地质, 1985, 3(2): 49–58.
- Yan Wenyuan. Characteristics of island arc type volcanics of early–middle Carboniferous and their mineral resources in the eastern Tianhan[J]. *Xinjiang Geology*, 1985, 3(2): 49–58 (in Chinese with English Abstract).
- [67] 罗婷, 廖群安, 陈继平, 等. 东天山雅满苏组火山岩LA–ICP–MS锆石U–Pb定年及其地质意义[J]. 地球科学——中国地质大学学报, 2012, 37(6): 1338–1352.
- Luo Ting, Liao Qunan, Chen Jiping, et al. LA–ICP–MS zircon U–Pb dating of the volcanic rocks from Yamansu formation in the Eastern Tianshan and its geological significance[J]. *Earth Science—Journal of China University of Geosciences*, 2012, 37(6): 1338–1352 (in Chinese with English abstract).
- [68] 杨富全, 刘锋, 柴凤梅, 等. 中国新疆阿尔泰铁矿床[M]. 北京: 地质出版社, 2012: 1–322.
- Yang Fuquan, Liu Feng, Chai Fengmei, et al. Altay Iron Deposits in Xinjing, China[M]. Beijing: Geological Publishing House, 2012: 1–322 (in Chinese with English abstract).
- [69] 张招崇, 侯通, 李厚民, 等. 岩浆热液系统中铁的富集机制探讨[J]. 岩石学报, 2014, 30(5): 1189–1204.
- Zhang Zhaocong, Hou Tong, Li Houming, et al. Enrichment mechanism of iron in magmatic–hydrothermal system[J]. *Acta Petrologica Sinica*, 2014, 30(5): 1189–1204 (in Chinese with English abstract).

Geochemistry and zircon U-Pb age of volcanic rocks from the Shaquanzi Fe-Cu deposit in East Tianshan Mountains and their geological significance

XU Lu-lu¹, CHAI Feng-mei¹, LI Qiang², ZENG Hong¹,
GENG Xin-xia², XIA Fang¹, DENG Gang³

(1. Xinjiang Key Laboratory for Geodynamic Processes and Metallogenetic Prognosis of the Central Asian Orogenic Belt, Xinjiang University, Urumqi 830049, Xinjiang, China; 2. Institute of Mineral Resources, Chinese Academy of Geological Sciences, Beijing 100037, China; 3. No. 6 Geological Party, Xinjiang Bureau of Geology and Mineral Resources, Hami 839000, Xinjiang, China)

Abstract: Located along the Aqishan-Yamansu belt of East Tianshan Mountains, the Shaquanzi Fe-Cu deposit is one of the deposits hosted in Paleozoic volcanic rocks. The deposit occurs in the second and third lithologic members of the Dikaner Formation consisting of volcanic rocks intercalated with sedimentary rocks. The iron mineralization also occurs at the contact zone between diorite-porphyrite and wall rocks. The tectonic setting and age of the volcanic rocks are key factors in the reconstruction of the ore-forming process. In this paper, representative samples of Dikaner Formation volcanic rocks and diorite-porphyrite in the Shaquanzi Fe-Cu ore district were analyzed for major and trace elements and zircon U-Pb dating was conducted to investigate the tectonic setting and formation ages of these rocks. LA-ICP-MS analyses of zircons with well-defined oscillatory zoning yielded mean $^{206}\text{Pb}/^{238}\text{U}$ ages of (321.7 ± 1.7) Ma and (322.7 ± 1.7) Ma, respectively, indicating that they were formed during late Early Carboniferous. The geochemical data suggest that most of the volcanic rocks belong to calc-alkaline series with the enrichment of LILE, LREE and depletion of Nb, Ta, and Ti, similar to the characteristics of arc volcanic rocks. The zircons from rhyolite and diorite-porphyrite have $\varepsilon_{\text{Hf}(0)}$ values of $+6.28 \sim +15.51$ and $-0.22 \sim +13.9$, respectively. The rhyolites were derived from juvenile crustal materials and basalts, which came from mantle wedge modified by fluids from subducted materials that formed andesite and diorite-porphyrite through crystal fractionation. Regional geology and geochemical evidence indicates that the Dikaner Formation volcanic rocks and diorite-porphyrite were formed simultaneously through island arc magmatism during the late stage of subduction. The Shaquanzi Fe-Cu deposit hosted in the Dikaner Formation were formed after 322 Ma.

Key words: volcanic rock; geochemistry; zircon U-Pb dating; Hf isotope; Shaquanzi Fe-Cu deposit, East Tianshan Mountains

About the first author: XU Lu-lu, female, born in 1989, master candidate, majors in mineralogy, petrology and economic geology; E-mail: 356725316@qq.com.

About the corresponding author: CHAI Feng-mei, female, born in 1971, professor, mainly engages in the teaching and study of petrology and economic geology; E-mail: chaifengmei@163.com.